

# Towards a precise prediction of the dark matter relic density within the MSSM

Julia Harz

ILP - LPTHE - UPMC - CNRS Paris

in collaboration with

B. Herrmann, M. Klasen, K. Kovarik, P. Steppeler

30/11/2016  
University of Oslo

J. Harz, B. Herrmann, M. Klasen, K. Kovářík, and P. Steppeler, Phys. Rev. D 93 114023 (2016)  
J. Harz, B. Herrmann, M. Klasen, K. Kovářík, and M. Meinecke, Phys. Rev D 91 034012 (2015)  
J. Harz, B. Herrmann, M. Klasen, K. Kovářík, Phys. Rev. D 91, 034028 (2015)  
J. Harz, B. Herrmann, M. Klasen, K. Kovářík, and Q. Le Bouc'h, Phys. Rev. D 87, 054031 (2013)



# I. Motivation & Introduction

# II. Processes & Technicalities

# III. Results & Phenomenology

# I. Motivation & Introduction

# What is Dark Matter?

There are ample hints for the existence of dark matter...

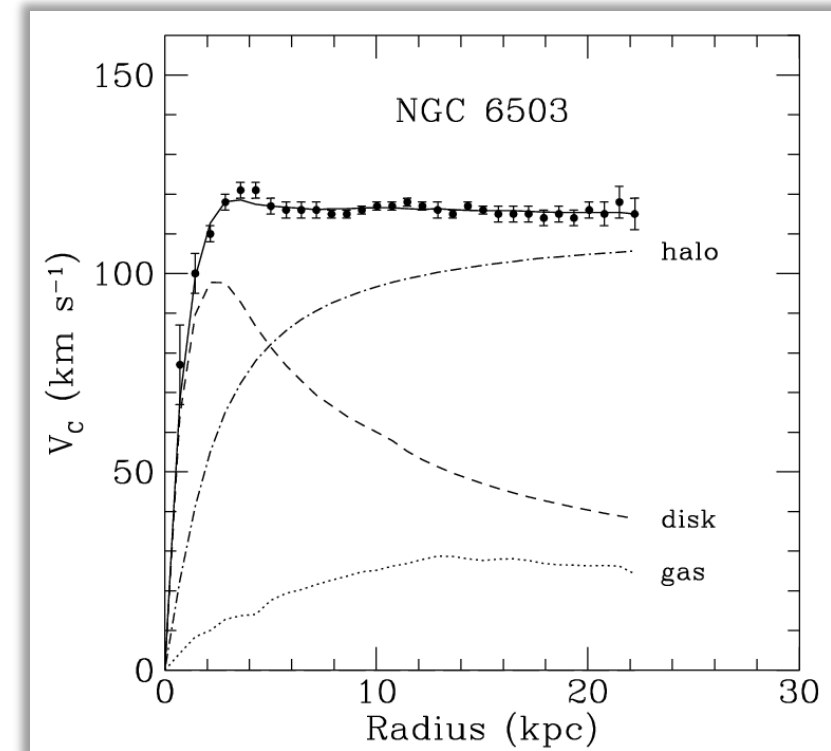
rotation curves of spiral galaxies

$$\text{circular velocity: } v_c(r) = \sqrt{\frac{GM(r)}{r}}$$

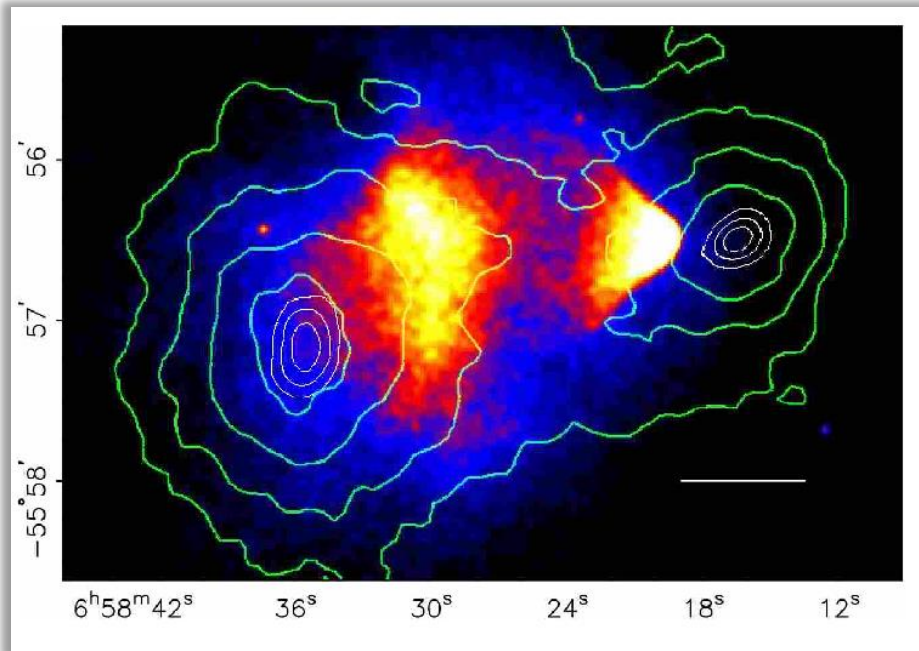
$$\text{with } M(r) = 4\pi \int_0^r dr' r'^2 \rho(r')$$

$$\text{expectation: } v_c(r) \propto 1/\sqrt{r}$$

$$\text{observation: } v_c(r) \propto \text{const.}$$



Begeman, Broeils, Sanders, MNRAS 249 (1991)



weak gravitational lensing effects of the Bullet Cluster

X-ray emission of colliding shock cones (yellow/red)



gravitational potential (green)

Clowe, Bradac, et al., The Astrophysical Journal 648 (2006)

# What is Dark Matter?

... which give us an idea of its characteristics and the possible theoretical model...

## DM characteristics

- non-baryonic
- stable
- neutral
- cold
- consistent with BBN
- consistent with stellar evolution

## Minimal Supersymmetric Standard Model (MSSM)

SM Particles		Spin		Spin		Superpartners
Quarks	$(u_L \ d_L)$	1/2	$Q$	0	$(\tilde{u}_L \ \tilde{d}_L)$	Squarks
	$u_R^\dagger$	1/2	$\bar{u}$	0	$\tilde{u}_R^*$	
	$d_R^\dagger$	1/2	$\bar{d}$	0	$\tilde{d}_R^*$	
Leptons	$(\nu \ e_L)$	1/2	$L$	0	$(\tilde{\nu} \ \tilde{e}_L)$	Sleptons
	$e_R^\dagger$	1/2	$\bar{e}$	0	$\tilde{e}_R^*$	
Higgs	$(H_u^+ \ H_u^0)$	0	$H_u$	1/2	$(\tilde{H}_u^+ \ \tilde{H}_u^0)$	Higgsinos
	$(H_d^0 \ H_d^-)$	0	$H_d$	1/2	$(\tilde{H}_d^0 \ \tilde{H}_d^-)$	
Gluon	$g$	1		1/2	$\tilde{g}$	Gluino
$W$ bosons	$W^0, W^\pm$	1		1/2	$\tilde{W}^0, \tilde{W}^\pm$	Winos
$B$ boson	$B^0$	1		1/2	$\tilde{B}^0$	Bino
Graviton	$G$	2		3/2	$\tilde{G}$	Gravitino

assuming conserved R-parity:  
lightest supersymmetric particle (LSP) stable

$$\mathcal{L} = -\frac{1}{2}(\psi^0)^T \mathcal{M}_{\tilde{\chi}^0} \psi^0 + h.c.$$

$$\psi^0 = (\tilde{B}, \tilde{W}^0, \tilde{H}_d^0, \tilde{H}_u^0)$$

$$\mathcal{M}_{\tilde{\chi}^0} = \begin{pmatrix} M_1 & 0 & -m_Z s_W c_\beta & m_Z s_W s_\beta \\ 0 & M_2 & m_Z c_W c_\beta & -m_Z c_W s_\beta \\ -m_Z s_W c_\beta & m_Z c_W c_\beta & 0 & -\mu \\ m_Z s_W s_\beta & -m_Z c_W s_\beta & -\mu & 0 \end{pmatrix}$$

accommodates naturally a good cold dark matter candidate: the lightest neutralino

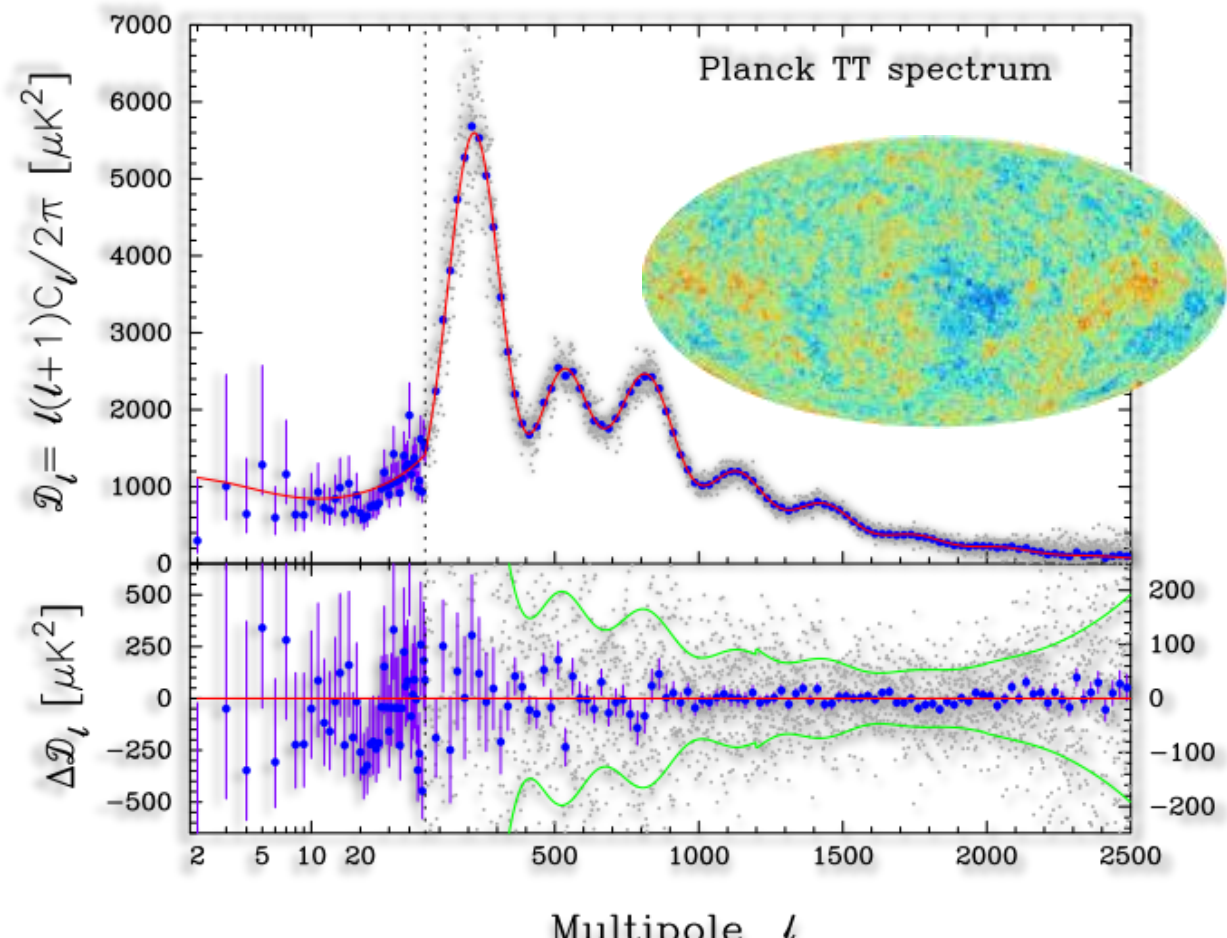
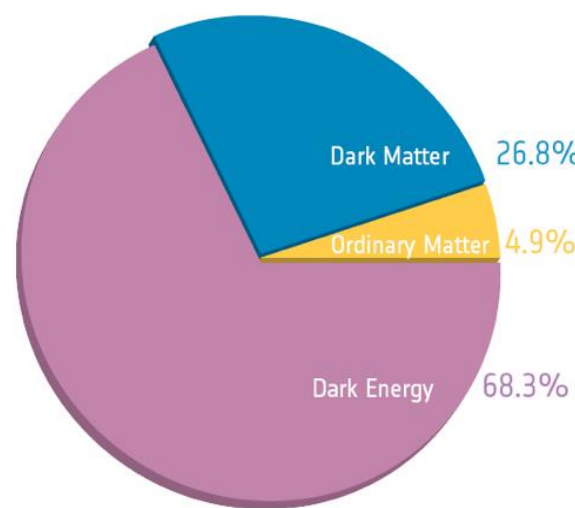
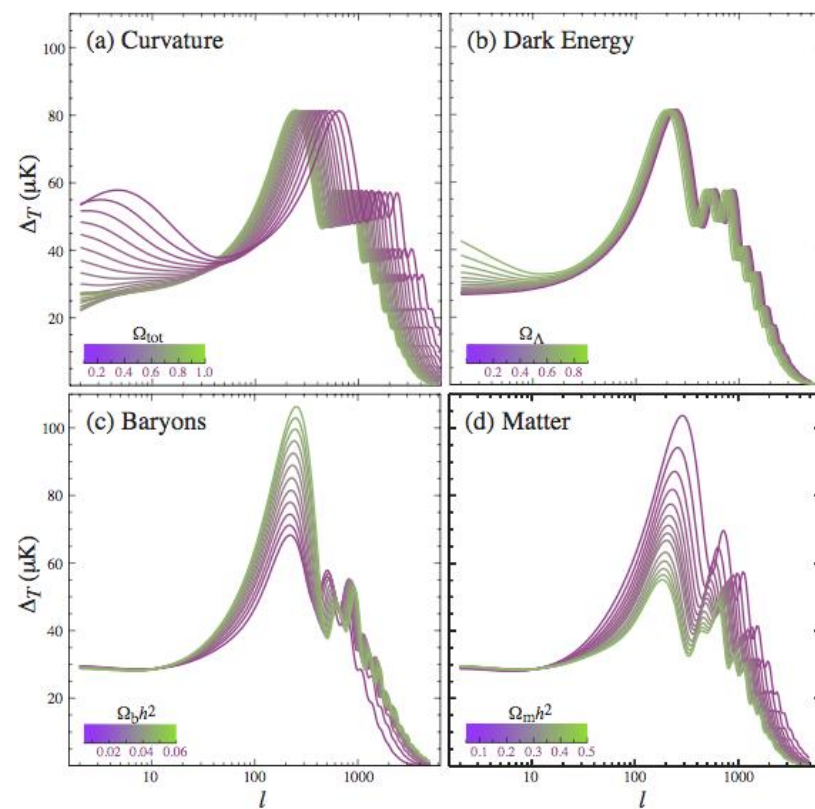
# Experimental Determination of the Relic Density

... also the amount of dark matter can be precisely determined...

- temperature fluctuations in the CMB can be described by 2-dimensional power spectrum

$$\frac{\delta T}{T}(\theta, \phi) = \sum_{l=2}^{+\infty} \sum_{m=-l}^{+l} a_{lm} Y_{lm}(\theta, \phi)$$

- assumption of a cosmological model ( $\Lambda$ CDM)
- fit of power spectrum possible



Planck Collaboration, arXiv:1303.5076

- baryonic density obtained to
- $$\Omega_b h^2 = 0.02222 \pm 0.00023$$
- dark matter density determined to

$$\Omega_{\text{CDM}} h^2 = 0.1199 \pm 0.0022$$

P. A. R. Ade et al. [Planck Collaboration], arXiv:1502.01589 [astro-ph.CO]

# Theoretical Prediction of the Relic Density

- number density of DM in the early universe can be described by the Boltzmann equation

$$\dot{n} + 3Hn = -\langle \sigma_{\text{eff}} v \rangle (n^2 - n_{\text{eq}}^2)$$

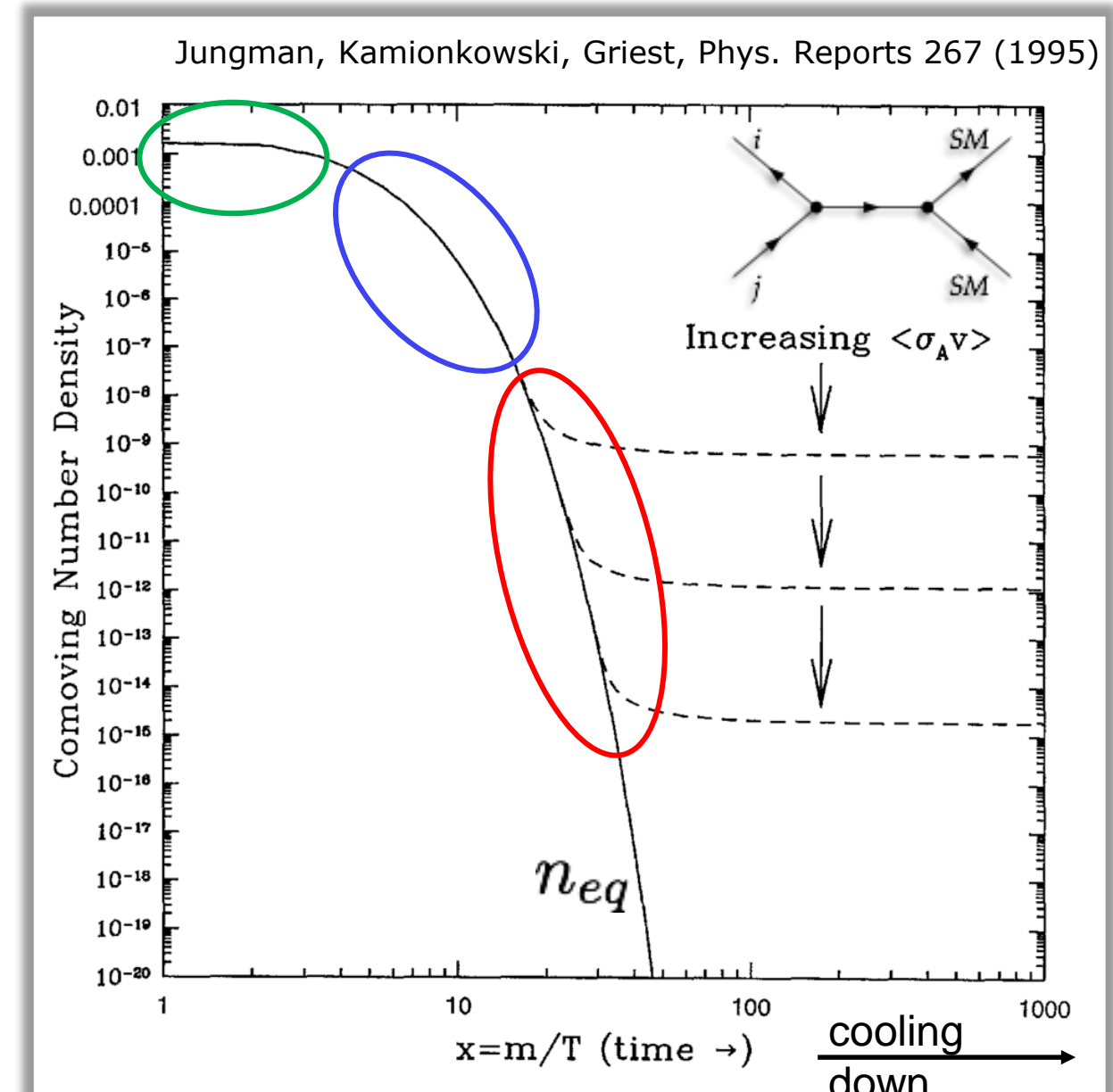
1) Thermal equilibrium regime ( $T >> m$ )  
annihilation and production of DM in thermal equilibrium

2) Annihilation regime ( $T \sim m/10$ )  
SM particles not energetic enough to create DM particles

3) Freeze-out ( $T \sim m/30$ )  
Annihilation rate falls behind expansion rate  $\rightarrow$  DM abundance

- relic density proportional to cross section

$$\Omega_\chi h^2 = \frac{n_\chi m_\chi}{\rho_{\text{crit}}} \propto \frac{1}{\langle \sigma_{\text{eff}} v \rangle}$$

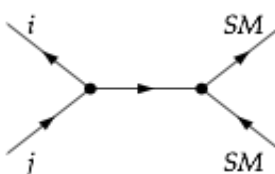


# Theoretical Prediction of the Relic Density

- number density of DM in the early universe can be described by the Boltzmann equation

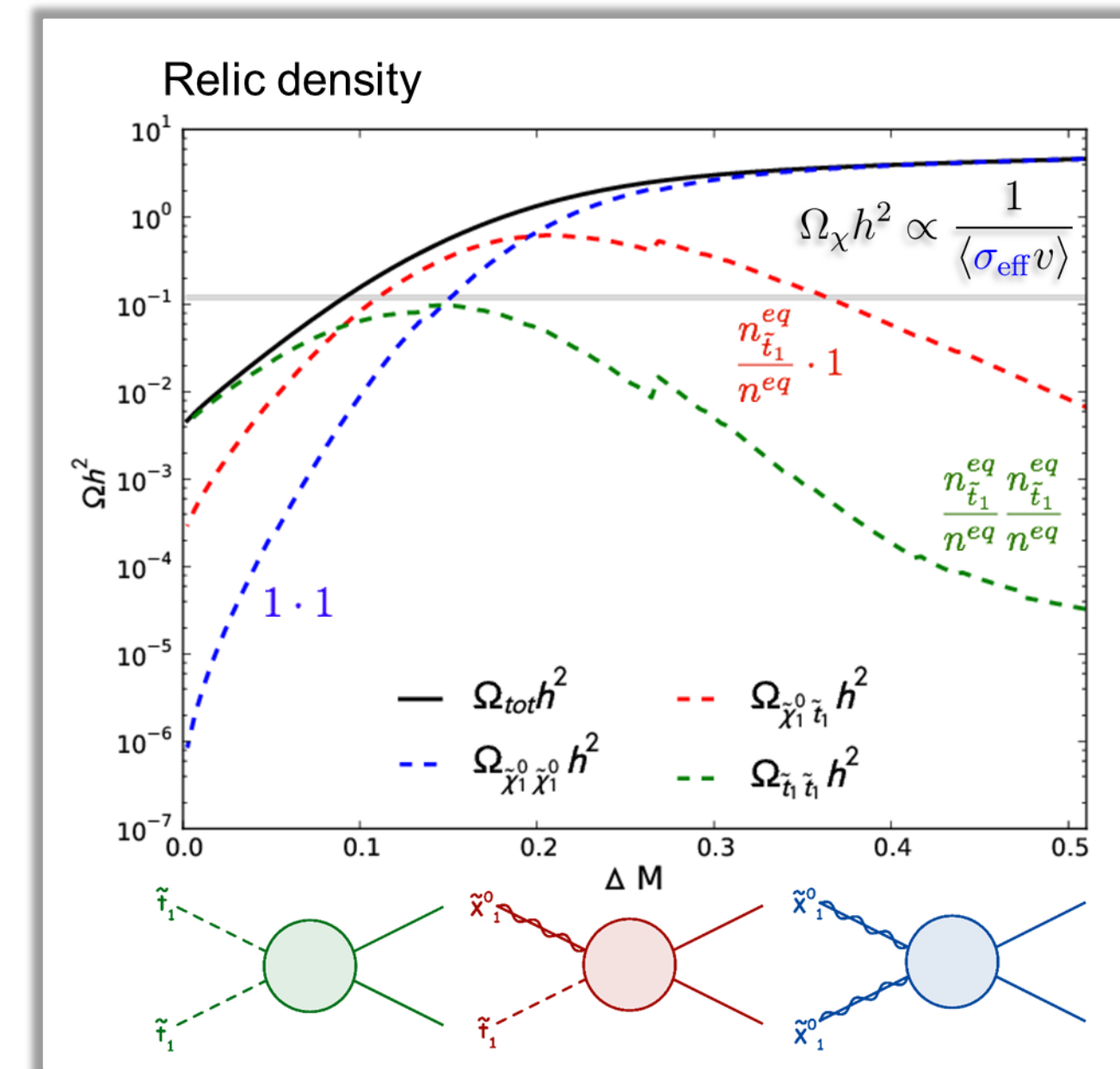
$$\dot{n} + 3Hn = -\langle \sigma_{\text{eff}} v \rangle (n^2 - n_{\text{eq}}^2)$$

$$\langle \sigma_{\text{eff}} v \rangle = \sum_{ij} \langle \sigma_{ij} v_{ij} \rangle \frac{n_i^{eq}}{n^{eq}} \frac{n_j^{eq}}{n^{eq}}$$



with  $\frac{n_i^{eq}}{n^{eq}} \propto \exp \frac{-(m_i - m_\chi)}{T} = \exp \frac{-(m_i - m_\chi)}{x m_\chi}$

- sizeable contributions of  $AB \rightarrow SM$  when particle A is almost degenerate in mass with particle B (DM candidate)
- dependent on mass difference various different processes can be important in the MSSM parameter space:
  - pair annihilation of neutralinos
  - coannihilation with other neutralinos, light stops, taus, etc...



we define  $\Delta M = \frac{m_{\tilde{t}_1} - m_{\tilde{\chi}_1}}{m_{\tilde{\chi}_1}}$

# Theoretical Prediction of the Relic Density

$$\dot{n} + 3Hn = -\langle \sigma_{\text{eff}} v \rangle (n^2 - n_{\text{eq}}^2)$$



$$\Omega_\chi h^2 \propto \frac{1}{\langle \sigma_{\text{eff}} v \rangle}$$

different relic density tools exist:

MicrOMEGAs

Belanger, Boudjema, et al. , CPC (2002)

DarkSUSY

Gondolo, Edsjö, et al. , JCAP (2004)

SuperIso Relic

Arbey, Mamoudi, et al. , CPC (2010)

MadDM

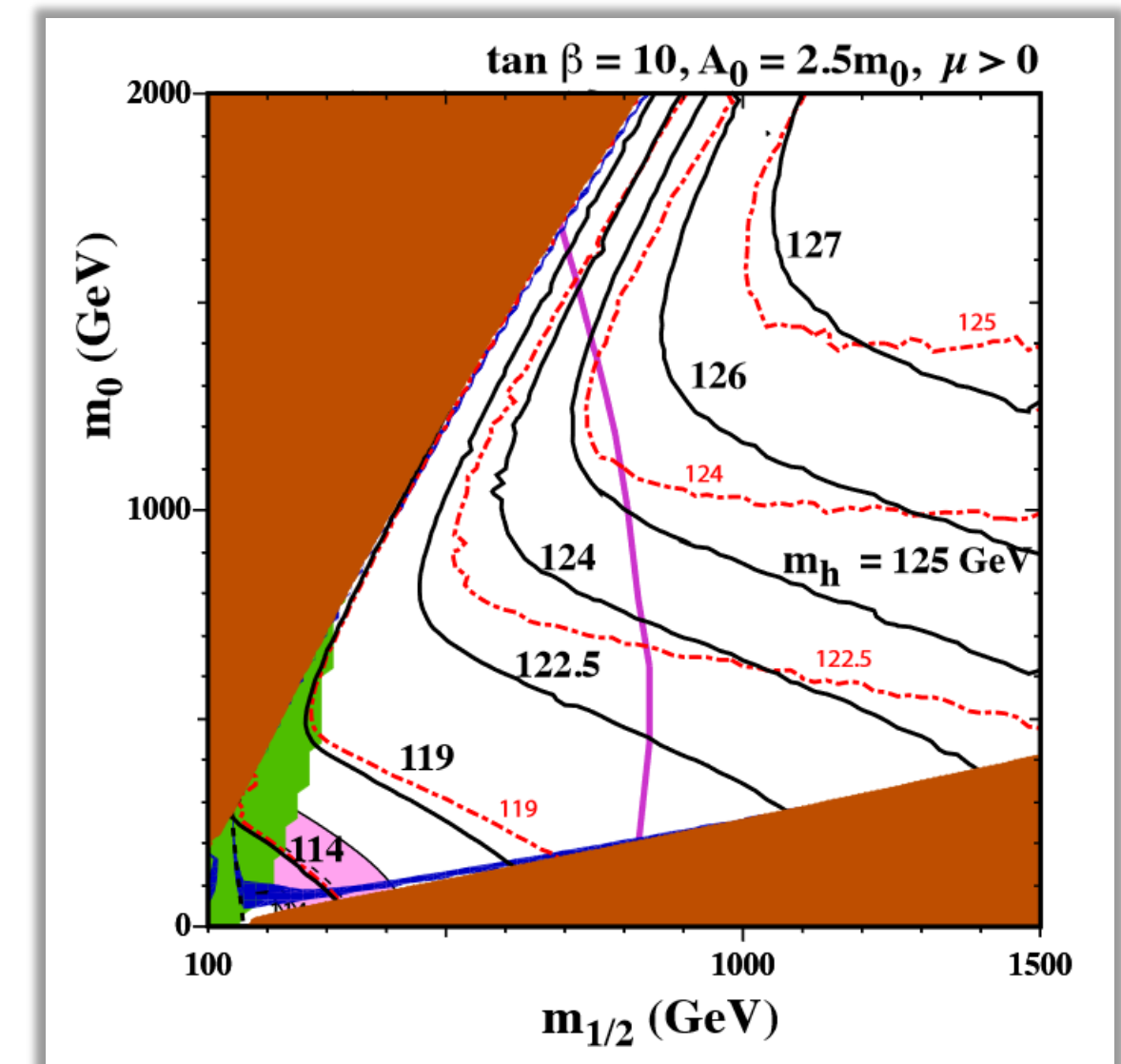
Backovic, Kong, et al. , (2013)

allows for constraining strongly the MSSM  
parameter space



Precision data from CMB measurements

PLANCK:  $\sim 1.5\%$  uncertainty



J. Ellis, K. Olive, J. Zheng, Eur. Phys. J. C74 (2014) 2947

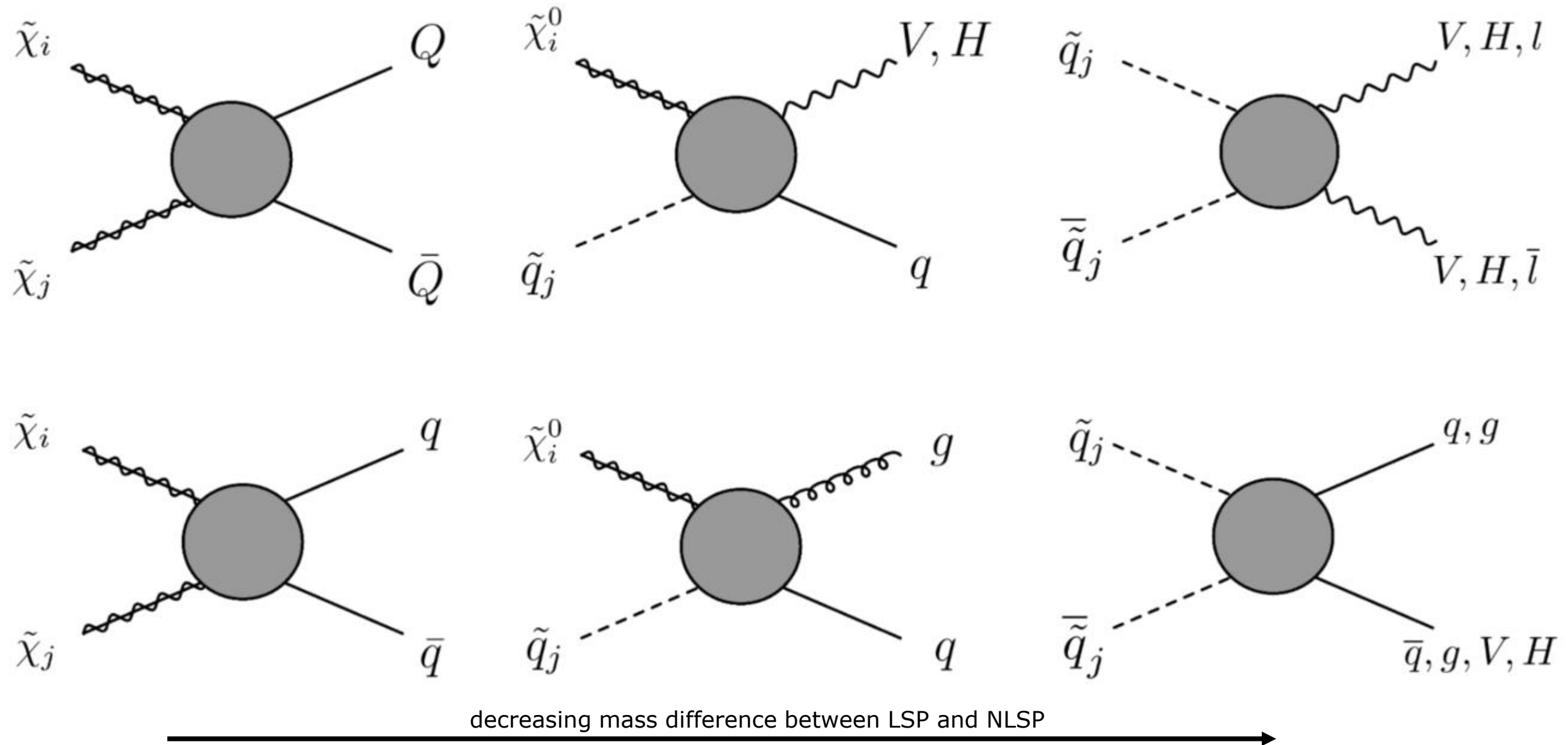
# Motivation to include Higher Order Corrections

1. Increased precision of relic density prediction by going to one-loop
2. Inclusion of significant Coulomb enhancement (resummation)
3. First study (at all!) of uncertainties coming from scale variation and
4. Scheme variation to the (co)annihilation cross section and the relic density

Tools do not take into account those three issues at all!

## II. Processes & Technicalities

# Calculation of SUSY-QCD NLO Corrections

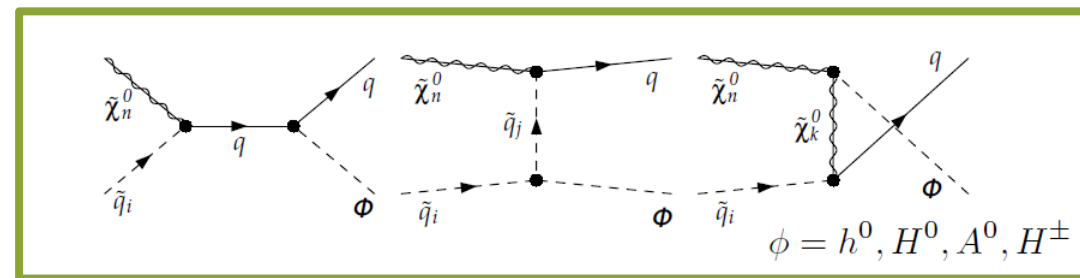


... and provide the results to public tools like micrOMEGAs

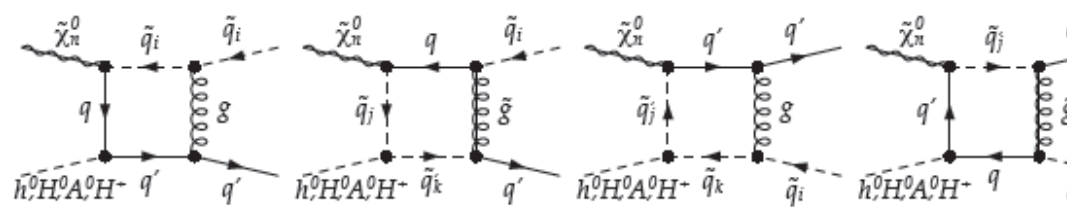
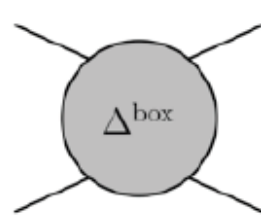
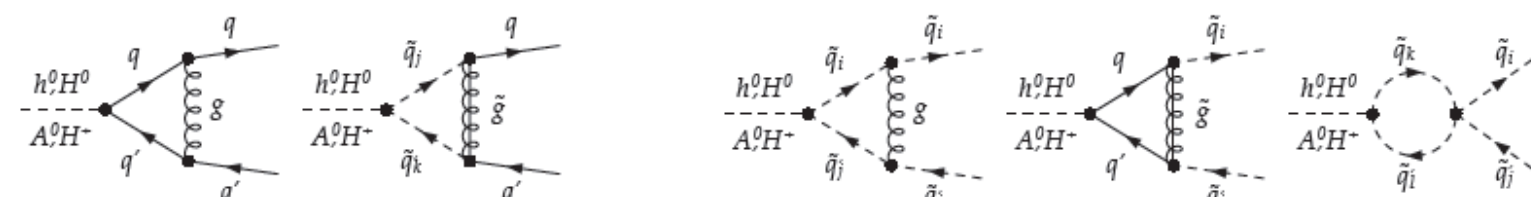
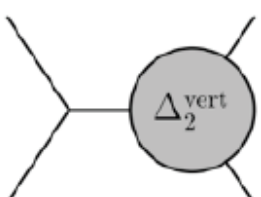
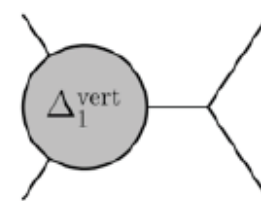
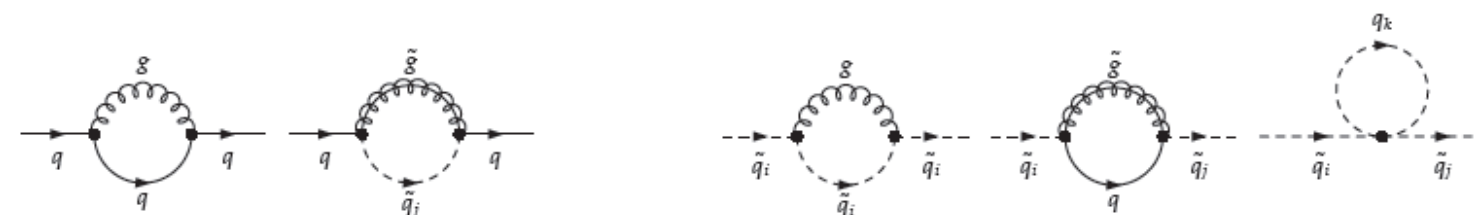
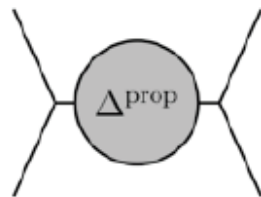
→ Aim 1 & 2: Increase precision!

# Recap: Loop Calculus in a Nutshell (I)

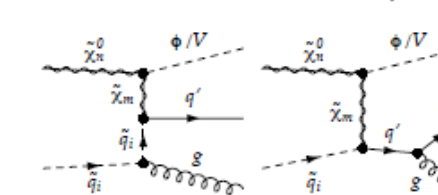
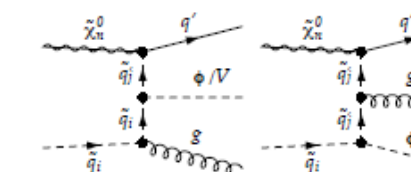
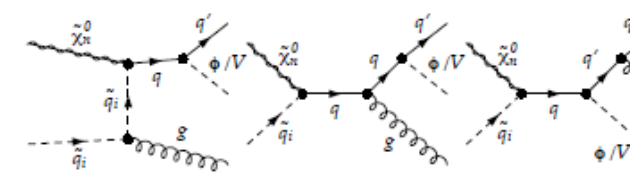
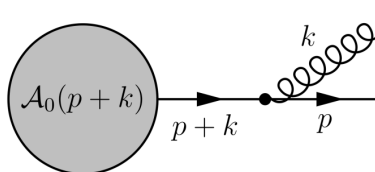
**Tree level:**



**NLO:**



virtual correction



real correction

~ 200 different diagrams

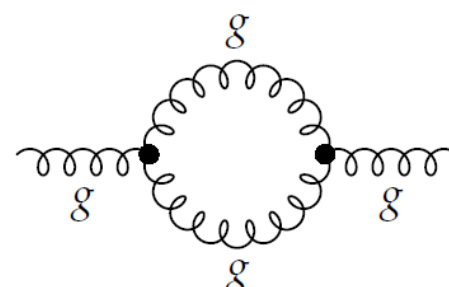
# Recap: Loop Calculus in a Nutshell (II)

## **Problem:** treatment of divergences

$$\sigma^{\text{NLO}} = \int_{2 \rightarrow 2} d\sigma^{\text{virtual}} + \int_{2 \rightarrow 3} d\sigma^{\text{real}} = \text{finite}$$

# Kinoshita-Lee-Lauenberg Theorem

## Dimensional regularisation:



$$\int_a^\infty \frac{1}{r^2} d^3r \quad - \text{ linear divergence} \quad \int_a^\infty \frac{1}{r^2} d^2r \quad - \text{ logarithmic divergence}$$

$\int_a^\infty \frac{1}{r^2} dr$  – converges

$$\int d^D q \frac{1}{(q^2)^2} = i(-1)^2 \frac{\pi^{D/2}}{\Gamma(\frac{D}{2})} \left( \int_0^{\mu^2} dq_E^2 (q_E^2)^{D/2-3} + \int_{\mu^2}^{\infty} dq_E^2 (q_E^2)^{D/2-3} \right)$$

$$= i(-1)^2 \frac{\pi^{D/2}}{\Gamma(\frac{D}{2})} \left( \frac{\mu^{D'-4}}{D' - 4} - \frac{\mu^{D-4}}{D - 4} \right) \quad \text{with } D' > 4 \text{ and } D < 4$$

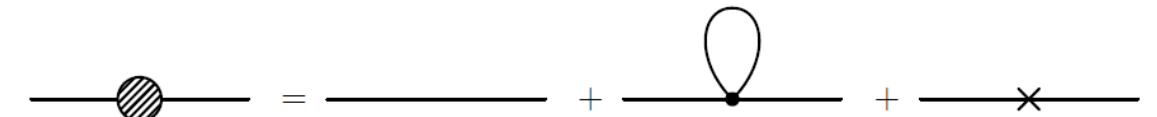
$$B_0(0,0,0) = \frac{1}{\epsilon_{\text{UV}}} - \frac{1}{\epsilon_{\text{IR}}} \quad \text{with } D = 4 - 2\epsilon$$


 renormalisation      cancellation with real corrections

## SUSY → Dimensional Reduction

# Recap: Loop Calculus in a Nutshell (III)

**UV- divergences → Renormalisation schemes**



$$\frac{i}{p^2 - m^2} + \frac{i}{p^2 - m^2} (-i\Sigma(p^2)) \frac{i}{p^2 - m^2} = \frac{i}{p^2 - m^2} \left(1 + \frac{\Sigma(p^2)}{p^2 - m^2}\right)$$

$$-i\Sigma(p^2) = -i\frac{\lambda}{2} \frac{1}{16\pi^2} A_0(m^2) + i[-m^2 \delta Z_m]$$

$$-i\Sigma(p^2) = -i\frac{\lambda}{2} \frac{m^2}{16\pi^2} \left[ \frac{1}{\varepsilon} - \gamma_E + \ln 4\pi - \ln \left( \frac{m^2 - i\epsilon}{\mu^2} + 1 \right) \right] - im^2 \delta Z_m.$$

**OS - scheme**

$$\text{Re } \Sigma(p^2) \Big|_{p^2=m^2} = 0 \quad \delta Z_m^{OS} = -\frac{\lambda}{32\pi^2} \left[ \Delta + 1 - \ln \left( \frac{m^2 - i\epsilon}{\mu^2} \right) \right]$$

$\Sigma(p^2) = 0$ , renormalised parameter fixed

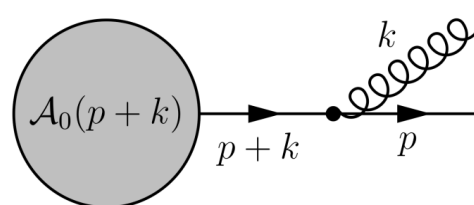
**DRbar - scheme**

$$\delta Z_m^{\overline{\text{DR}}} = -\frac{\lambda}{32\pi^2} \Delta$$

$$\Sigma(p^2) = \frac{\lambda m^2}{32\pi^2} \left[ 1 - \ln \left( \frac{m^2 - i\epsilon}{\mu^2} \right) \right]$$

renormalised parameter scale dependent

**IR-divergences → soft & collinear divergences**



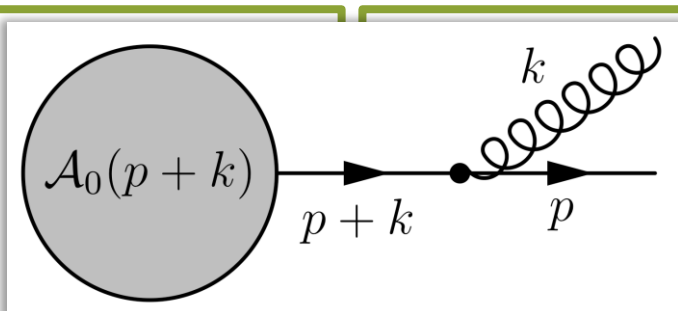
$$\frac{1}{(p+k)^2 - m^2} = \frac{1}{2p \cdot k} = \frac{1}{\omega(E_p - |\vec{p}| \cos \theta)} \xrightarrow[m_p=0 \wedge \theta \rightarrow 0]{\omega \rightarrow 0 \vee} \infty$$

**soft**

**collinear**

# Infrared Treatment

## Dipole subtraction



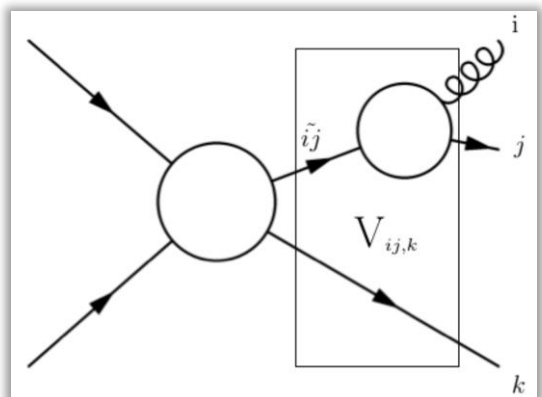
- auxiliary cross section  $d\sigma^A$  is introduced = local counter term
- three-particle and two-particle phase space separately finite

$$\sigma_{\text{NLO}} = \int_3 \left[ d\sigma^R \Big|_{\epsilon=0} - d\sigma^A \Big|_{\epsilon=0} \right] + \int_2 \left[ d\sigma^V + \int_1 d\sigma^A \right]_{\epsilon=0}$$

- general structure of  $d\sigma^A$  given as

$$\begin{aligned} |M^A|^2 &= \sum_{i,j} \sum_{k \neq i,j} \mathcal{D}_{ijk} \\ &= \sum_{i,j} \sum_{k \neq i,j} V_{ij,k}(p_i, \tilde{p}_{ij}, \tilde{p}_k) \otimes |M^B(\tilde{p}_{ij}, \tilde{p}_k)|^2 \end{aligned}$$

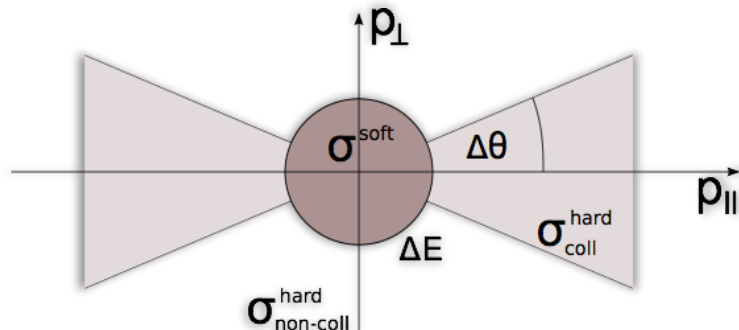
- $V_{ij,k}$  becomes proportional to Altarelli-Parisi splitting functions in collinear limit and to eikonal factors in the soft limit



S. Catani et al. Nucl. Phys. B 627 (2002), S. Catani, M.H. Seymour, Phys. Lett. B 378 (1996)  
S. Catani, M.H. Seymour Nucl. Phys. B 485 (1997), S. Dittmaier, Nucl. Phys. B 565 (2000)

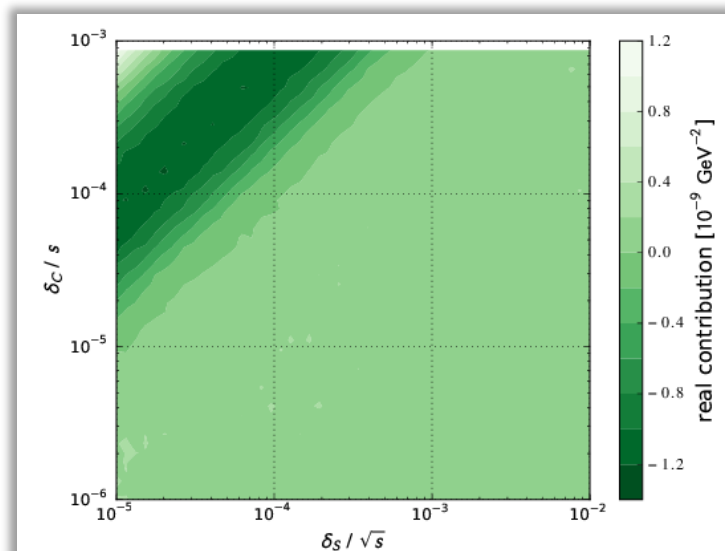
## Phase space slicing

- phase space is sliced into regions of different divergent classes
- approximations allow for analytical integration

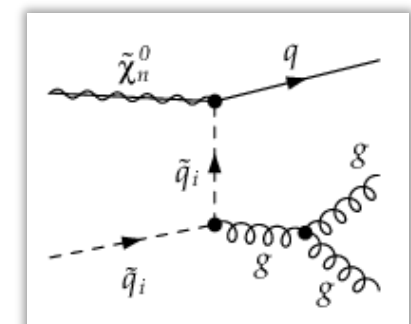


$$\sigma^{real} = \sigma^{\text{soft}}(\Delta E) + \sigma^{\text{hard}}(\Delta E, \Delta \theta) + \sigma^{\text{hard non-coll}}(\Delta E, \Delta \theta)$$

eikonal                          hard-collinear                          pure  $2 \rightarrow 3$   
approximation    approximation                          processes



B. W. Harris, J. F. Owens, Phys. Rev. D65 (2002)



# Renormalisation I

Renormalisation scheme has to be valid over a wide parameter space for all (co)annihilation processes

- relevant parameters:  $m_{\tilde{t}_1}, m_{\tilde{t}_2}, m_{\tilde{b}_1}, m_{\tilde{b}_2}, m_t, m_b, A_t, A_b, \theta_{\tilde{t}}, \theta_{\tilde{b}}$

known masses  
relevant as incoming  
(co)annihilating particles

crucial for coannihilating scenarios;  
as dependent parameter problem of  
large effects for large tanbeta

- hybrid on-shell /  $\overline{\text{DR}}$  renormalisation scheme

$$m_{\tilde{t}_1}^{\text{OS}}, m_{\tilde{b}_1}^{\text{OS}}, m_{\tilde{b}_2}^{\text{OS}} \quad A_t^{\overline{\text{DR}}}, A_b^{\overline{\text{DR}}} \quad m_t^{\text{OS}}, m_b^{\overline{\text{DR}}}$$

input parameters

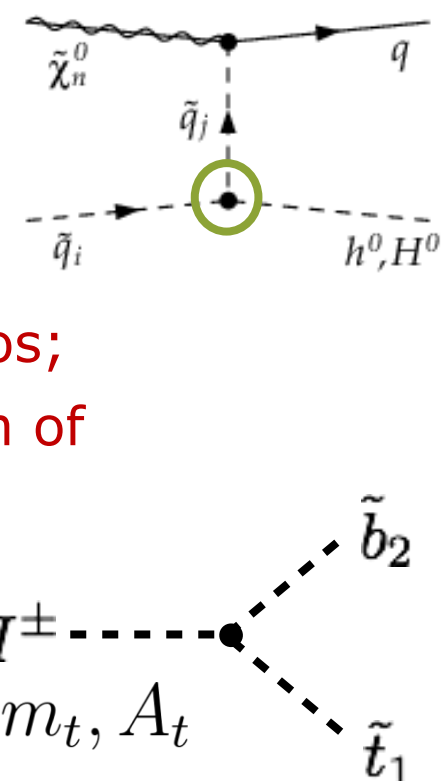


$$m_{\tilde{t}_2}, \theta_{\tilde{t}}, \theta_{\tilde{b}}$$

dependent parameters

$$\begin{pmatrix} m_{\tilde{q}_1}^2 & 0 \\ 0 & m_{\tilde{q}_2}^2 \end{pmatrix} = U^{\tilde{q}} \begin{pmatrix} M_{\tilde{Q}}^2 + (I_q^{3L} - e_q s_W^2) \cos 2\beta m_Z^2 + m_q^2 & m_q (A_q - \mu (\tan \beta)^{-2I_q^{3L}}) \\ m_q (A_q - \mu (\tan \beta)^{-2I_q^{3L}}) & M_{\{\tilde{U}, \tilde{D}\}}^2 + e_q s_W^2 \cos 2\beta m_Z^2 + m_q^2 \end{pmatrix} (U^{\tilde{q}})^\dagger$$

→ Aim 4: Study dependence on renormalisation scheme!



# Renormalisation II

- bottom quark mass

$$m_b^{\text{SM},\overline{\text{MS}}}(m_b) \xrightarrow{(1)} m_b^{\text{SM},\overline{\text{MS}}}(Q) \xrightarrow{(2)} m_b^{\text{SM},\overline{\text{DR}}}(Q) \xrightarrow{(3)} m_b^{\text{MSSM},\overline{\text{DR}}}(Q)$$

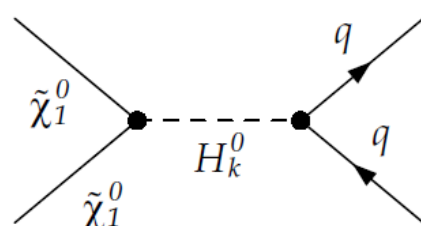
3-loop RGEs                    2-loop relation                    2-loop threshold corrections

K.G Chetyrkin, Phys. Lett. B 404, 161 (1997)    R. Harlander, et al. JHEP 0609, 053 (2006)    A. Bauer et al., JEP 0902, 03 (2009)  
A. Bauer et al., JEP 0902, 03 (2009)

- bottom Yukawa coupling

$$[(h_b^{\overline{\text{MS}},\text{QCD},\Phi})(Q)]^2 = [(h_b^{\overline{\text{MS}},\Phi})(Q)]^2 [1 + \Delta_{\text{QCD}} + \Delta_t^\Phi]$$

effective Yukawa couplings with QCD  
corrections and top-quark induced  
contributions...



K.G Chetyrkin, Phys. Lett. B 390, 309 (1997)  
P.A.Baikov et al. Phys. Rev. Lett. 96, 012003 (2006)  
K.G. Chetyrkin et al. Nucl. Phys. B 461, 3 (1996)

$$\begin{aligned} h_b^{\text{MSSM},h}(Q) &= \frac{h_b^{\overline{\text{MS}},\text{QCD},h}(Q)}{1 + \Delta_b} \left[ 1 - \frac{\Delta_b}{\tan \alpha \tan \beta} \right], \\ h_b^{\text{MSSM},H}(Q) &= \frac{h_b^{\overline{\text{MS}},\text{QCD},H}(Q)}{1 + \Delta_b} \left[ 1 + \Delta_b \frac{\tan \alpha}{\tan \beta} \right], \\ h_b^{\text{MSSM},A}(Q) &= \frac{h_b^{\overline{\text{MS}},\text{QCD},A}(Q)}{1 + \Delta_b} \left[ 1 - \frac{\Delta_b}{\tan^2 \beta} \right] \end{aligned}$$

...and resummed  $\Delta_b$  important for large  
 $\tan \beta$  effects

M. Carena et al., Nucl. Phys. B 577, 88 (2000)  
J. Guasch et al., Phys. Rev. D 68 115001 (2003)  
D. Noth and M. Spira, JHEP 1106, 084 (2011)

- strong coupling constant

$$\alpha_s^{\overline{\text{MS}},\text{SM},n_q=5}(m_Z^2) \xrightarrow{(1)} \alpha_s^{\overline{\text{MS}},\text{SM},n_q=5}(Q^2) \xrightarrow{(2)} \alpha_s^{\overline{\text{DR}},\text{SM},n_q=5}(Q^2) \xrightarrow{(3)} \alpha_s^{\overline{\text{DR}},\text{MSSM},n_q=6}(Q^2)$$

3-loop RGEs                    2-loop relation                    2-loop threshold corrections

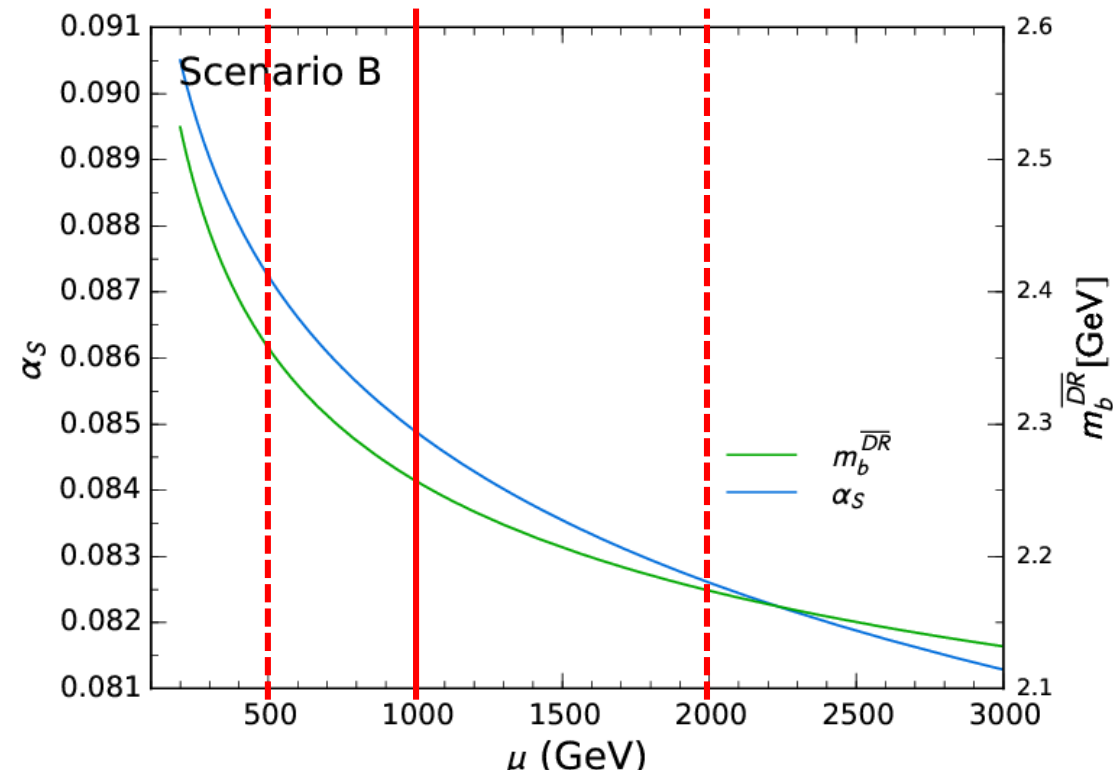
J. Vermaseren et al., Phys. Lett. B 405, 327 (1997)    R. Harlander, et al. Phys. Rev. D 72 095009 (2005)    A. Bauer et al., JEP 0902, 03 (2009)

# Theoretical Uncertainty from Scale Variation

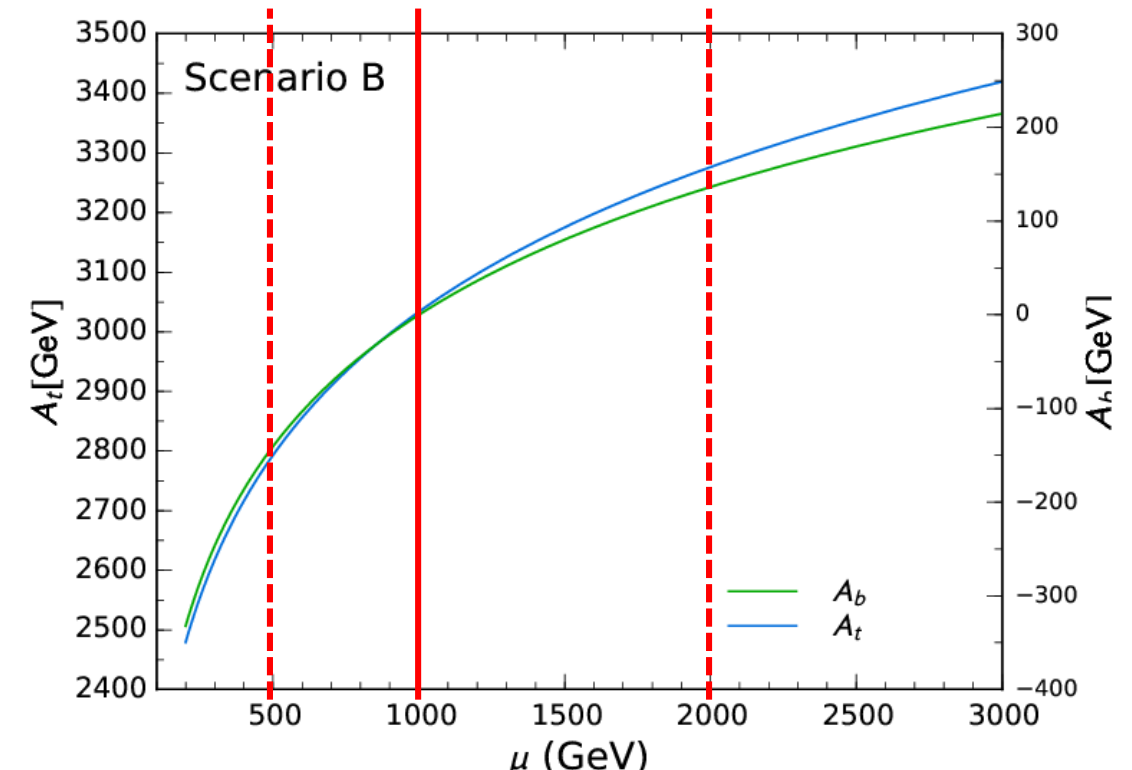
- loop calculation contains explicit uncancelled logs of the renormalisation scale
- is implicitly dependent on scale dependent parameters  $\alpha_s, \theta_{\tilde{t}}, \theta_{\tilde{b}}, A_t, A_b, m_b, m_{\tilde{t}_2}$

→ scale variation gives an estimate of the uncertainty of the calculation

$$\frac{1}{2}\mu_R < \mu < 2\mu_R$$



$\alpha_s$  less scale dependent as in TeV range



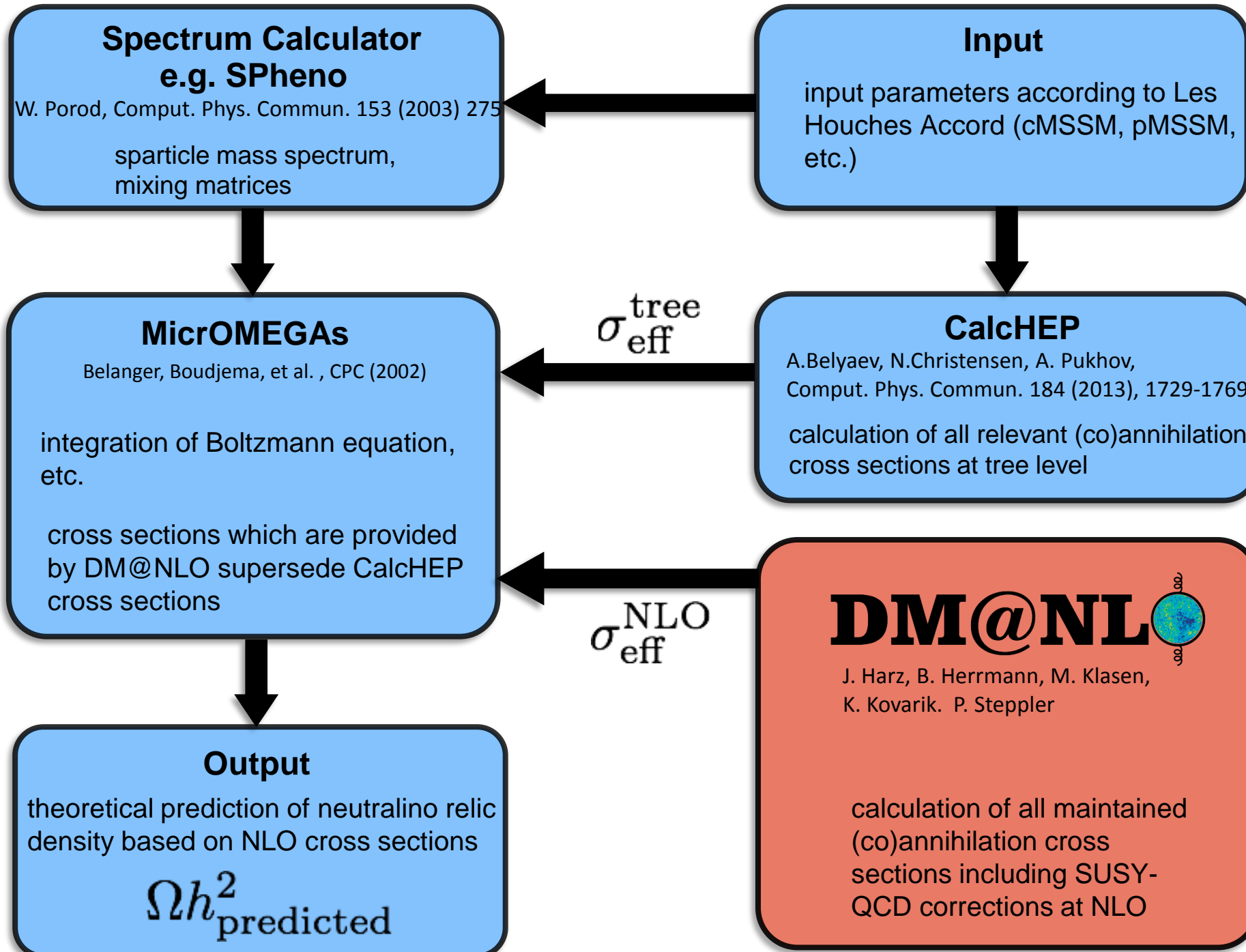
trilinear couplings more scale dependent

→ Aim 3: Study dependence on renormalisation scale!

→ first study in literature!

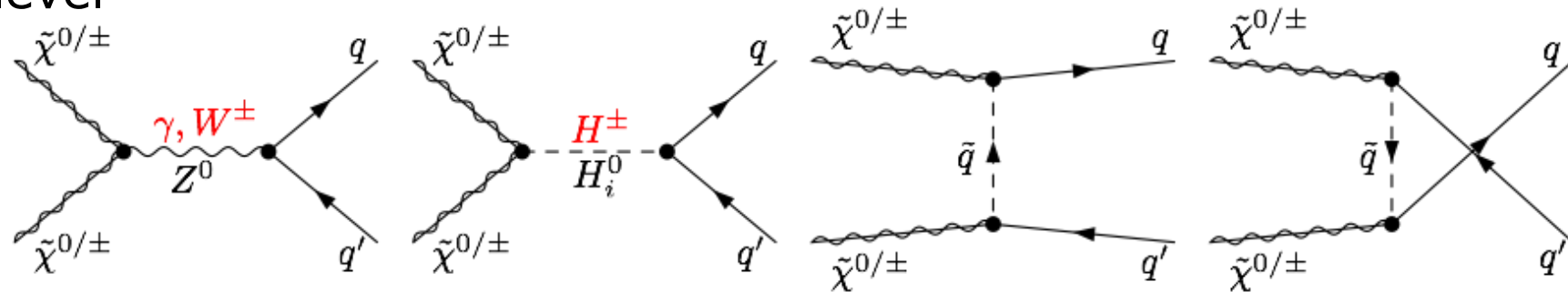
# III. Results & Phenomenology

# Performing Parameter Studies

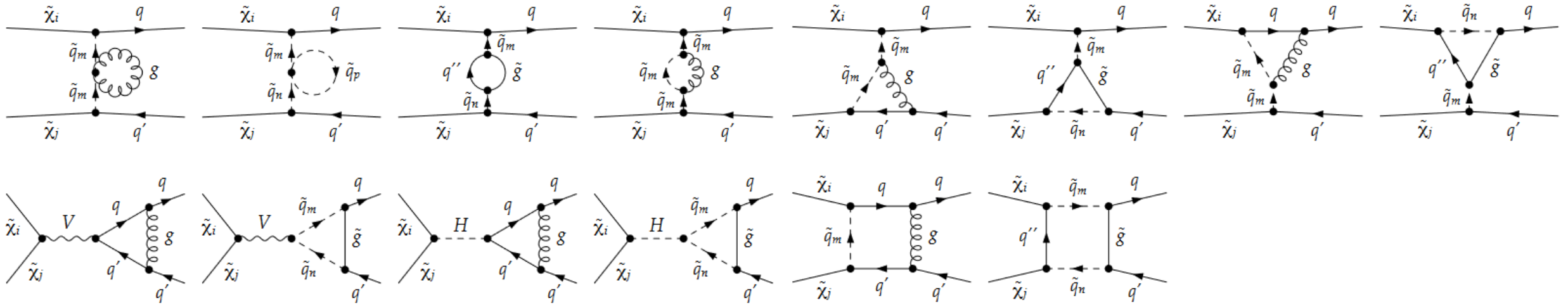


# Gaugino Annihilation

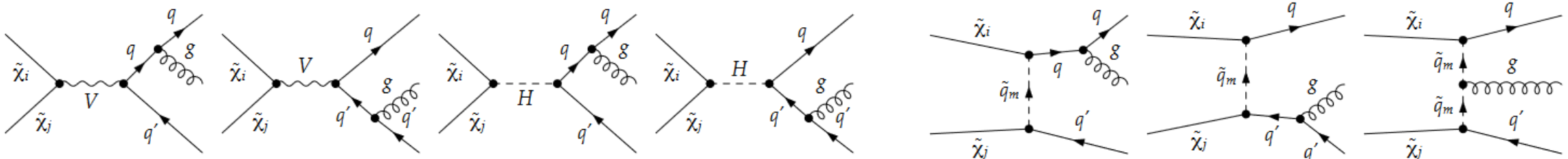
Tree level



Virtual one-loop corrections

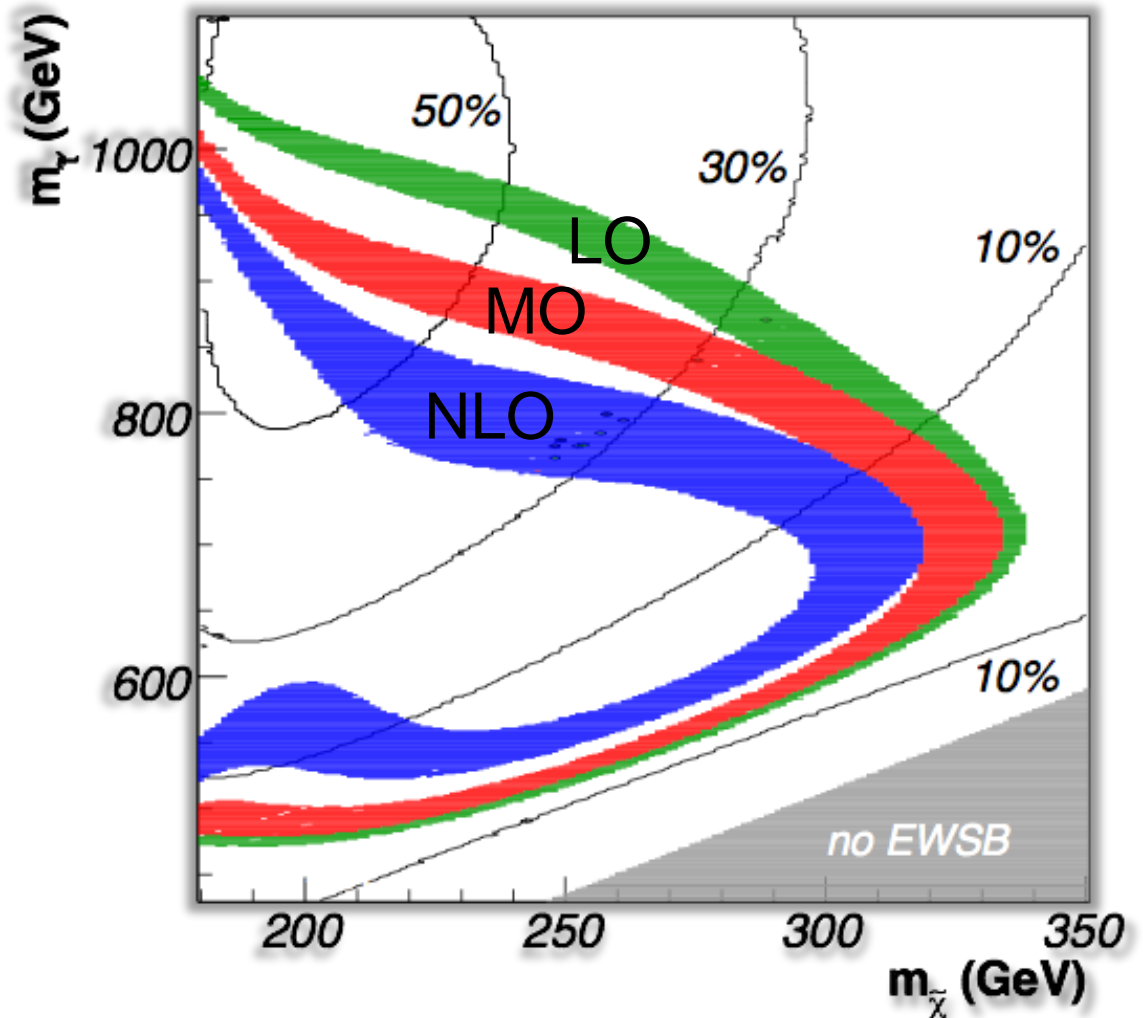
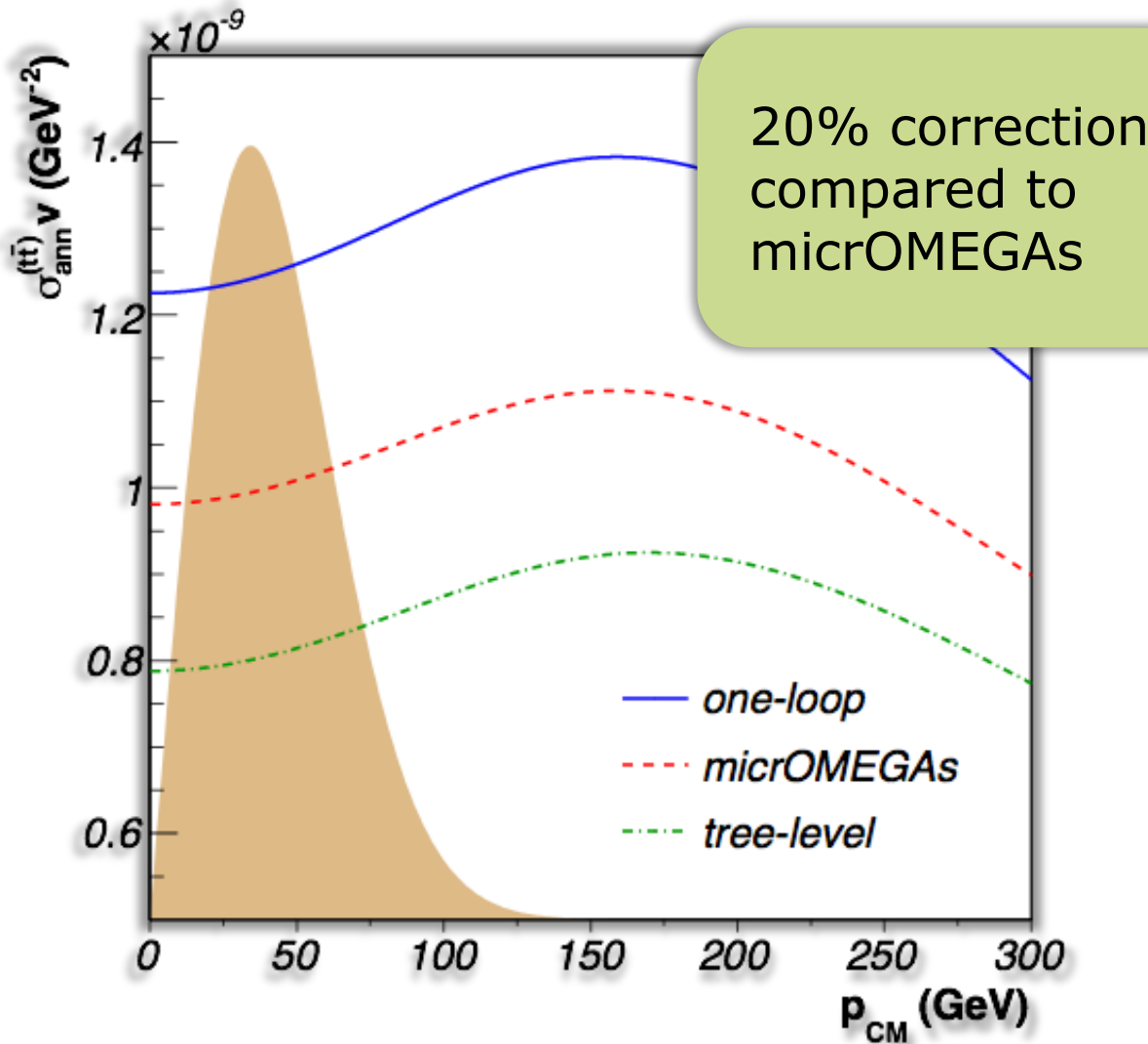
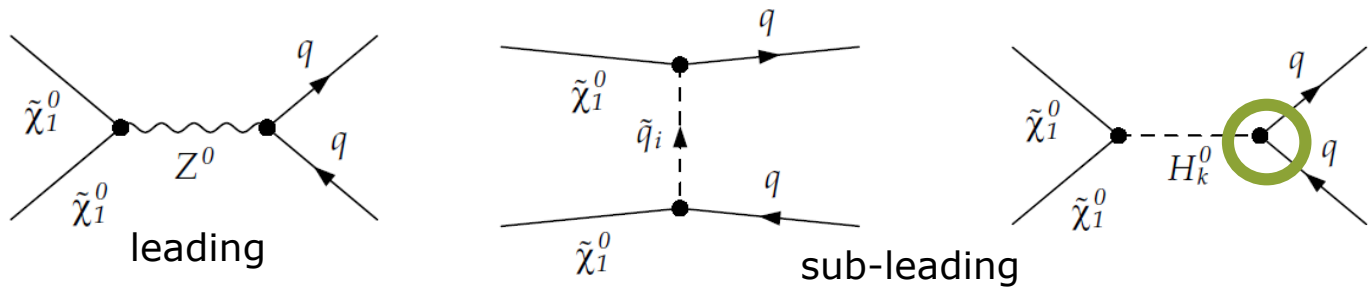


Real gluon emission processes



# Neutralino Annihilation

- Example: Dominant Z-exchange



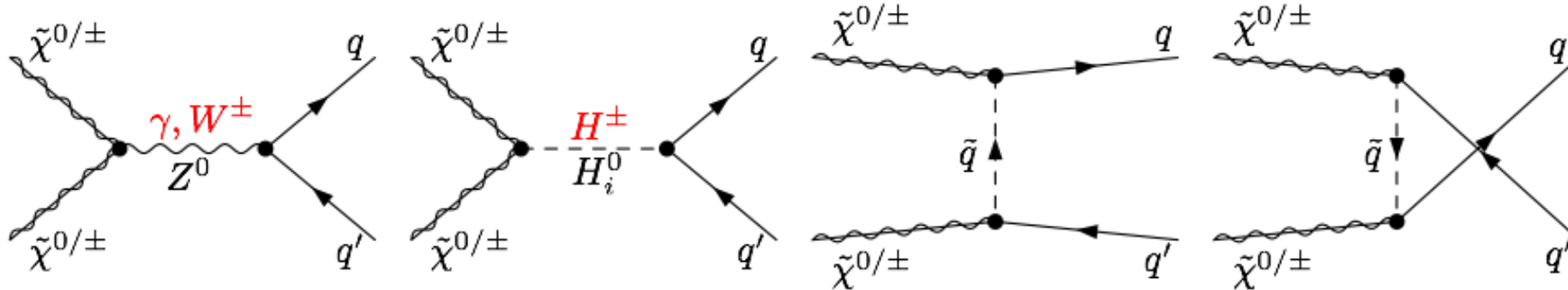
- effective Yukawa couplings not always sufficient, e.g. for dominant Z-exchange

→ shift of about 100 GeV in physical mass plane

B. Herrmann, M. Klasen and K. Kovařík, Phys. Rev. D 79: 061701 (2009), arXiv:0901.0481 [hep-ph]  
 B. Herrmann, M. Klasen and K. Kovařík, Phys. Rev. D 80: 085025 (2009), arXiv:0907.0030 [hep-ph]

# Gaugino Annihilation

Tree level

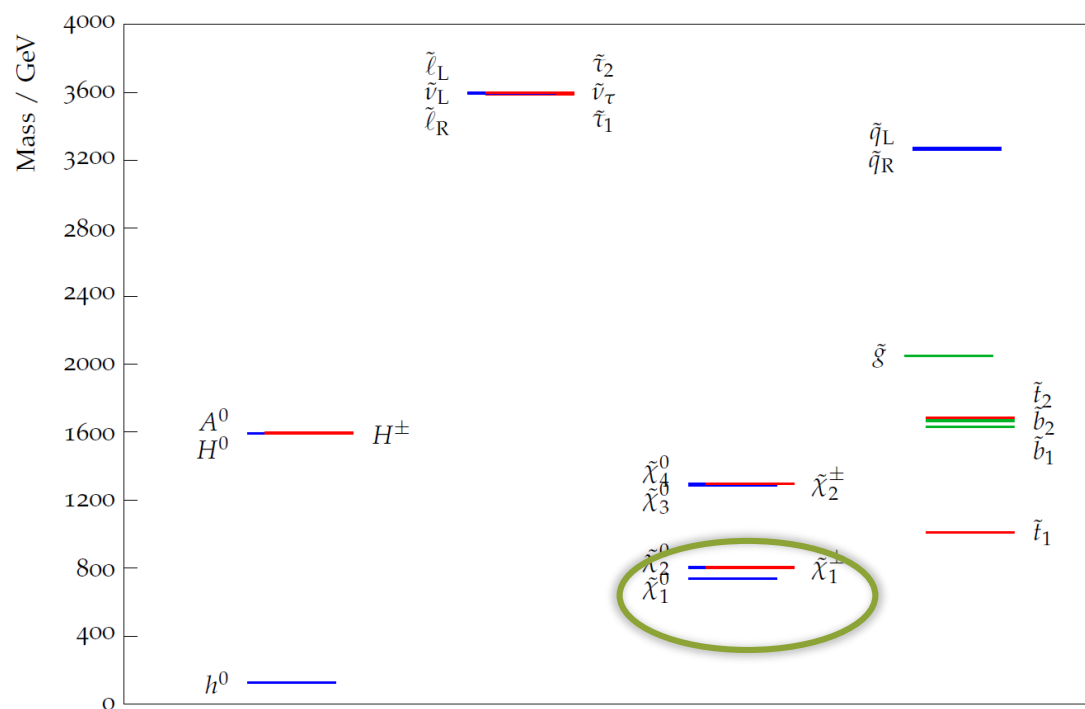


Input parameter pMSSM11

$\tan \beta$	$\mu$	$m_A$	$M_1$	$M_2$	$M_3$	$M_{\tilde{q}_{1,2}}$	$M_{\tilde{q}_3}$	$M_{\tilde{u}_3}$	$M_{\tilde{\ell}}$	$A_t$
13.4	1286.3	1592.9	731.0	766.0	1906.3	3252.6	1634.3	1054.4	3589.6	-2792.3

Masses, mixing & observables

	$m_{\tilde{\chi}_1^0}$	$m_{\tilde{\chi}_2^0}$	$m_{\tilde{\chi}_1^\pm}$	$m_{\tilde{\chi}_2^\pm}$	$m_{\tilde{t}_1}$	$m_{\tilde{t}_2}$	$Z_{1\tilde{B}}$	$Z_{1\tilde{W}}$	$Z_{1\tilde{H}_1}$	$Z_{1\tilde{H}_2}$	$m_h^0$	$\Omega_{\tilde{\chi}_1^0} h^2$	$\text{BR}(b \rightarrow s\gamma)$
A	738.1	802.5	802.4	1295.3	1032.1	1682.0	-0.996	0.049	-0.059	0.037	126.5	0.1248	$3.0 \cdot 10^{-4}$



	A
$\tilde{\chi}_1^0 \tilde{\chi}_1^0 \rightarrow t\bar{t}$	2%
$\tilde{\chi}_1^0 \tilde{\chi}_1^0 \rightarrow b\bar{b}$	9%
$\tilde{\chi}_1^0 \tilde{\chi}_2^0 \rightarrow t\bar{t}$	3%
$\tilde{\chi}_1^0 \tilde{\chi}_2^0 \rightarrow b\bar{b}$	23%
$\tilde{\chi}_1^0 \tilde{\chi}_1^\pm \rightarrow t\bar{b}, \bar{t}b$	43%
Total	80%

$$m_{\tilde{\chi}_1^0} + m_{\tilde{\chi}_1^+} = 1540.5 \text{ GeV}$$

$$m_{\tilde{\chi}_1^0} + m_{\tilde{\chi}_2^0} = 1540.6 \text{ GeV}$$

$$2m_{\tilde{\chi}_1^0} = 1476.4 \text{ GeV}$$

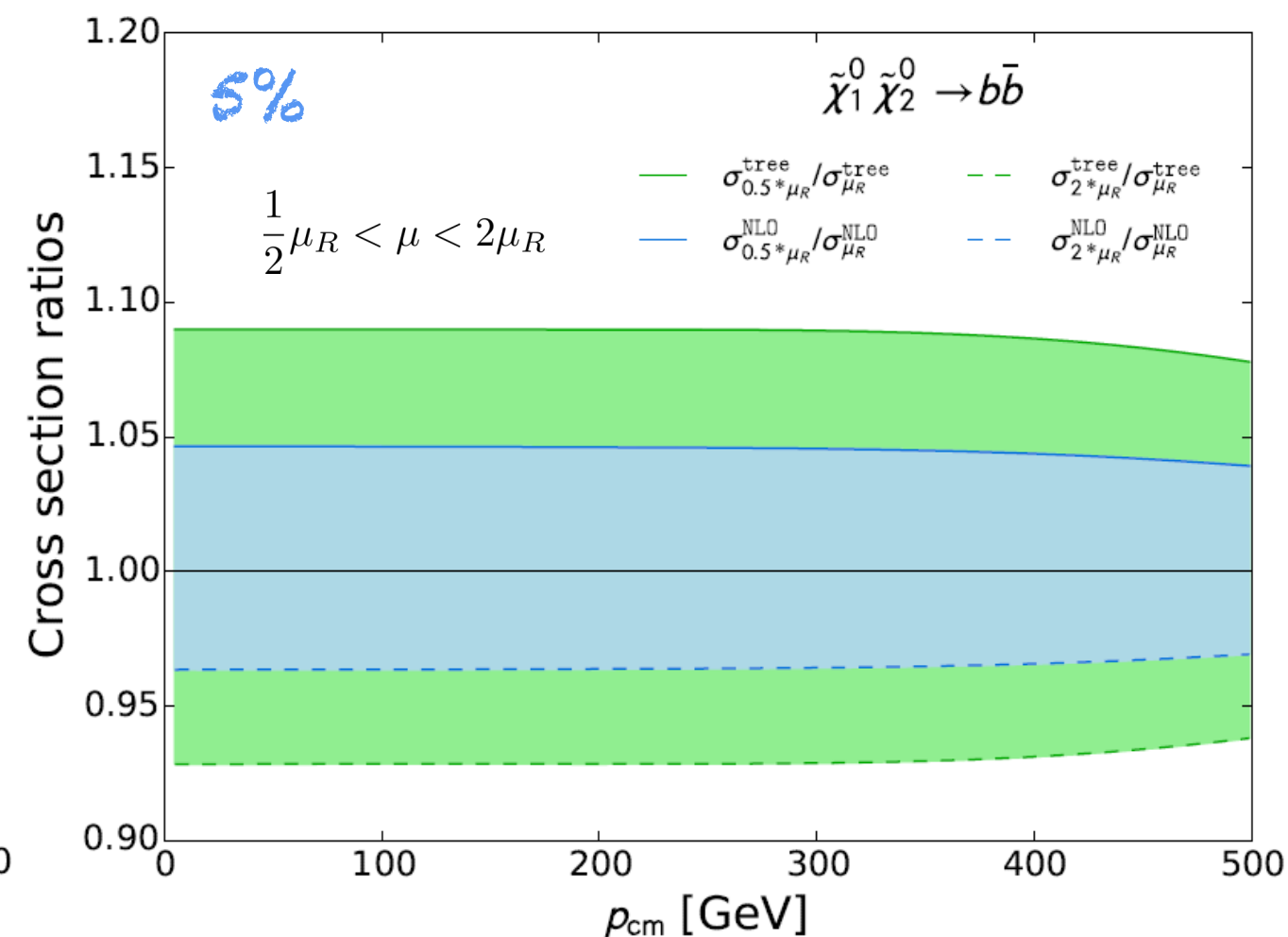
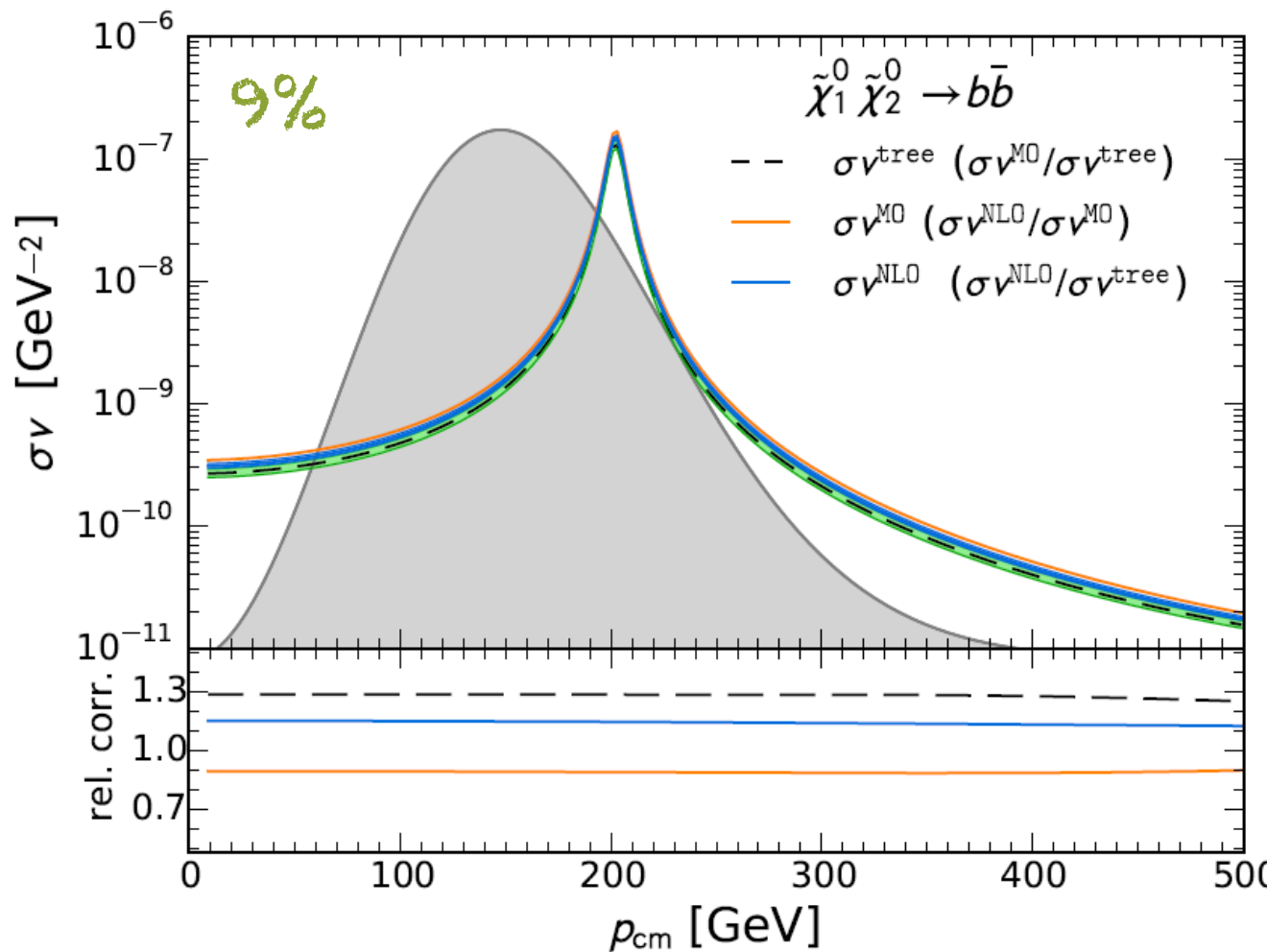
$$2m_{\tilde{\chi}_2^0} \approx 2m_{\tilde{\chi}_1^+} \approx 1600 \text{ GeV}$$

$$m_{H^\pm} = 1595.1 \text{ GeV}$$

$$m_{A^0} = 1592.9 \text{ GeV}$$

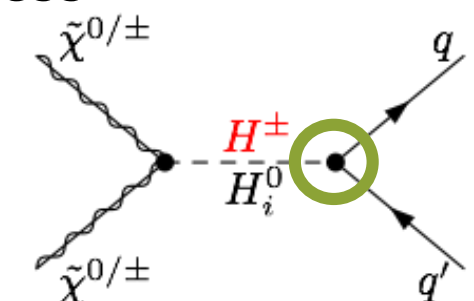
J. Harz, B. Herrmann, M. Klasen, K. Kovařík, and P. Steppeler, arXiv:1602.08103 [hep-ph]  
 B. Herrmann, M. Klasen, K. Kovařík, M. Meinecke and P. Steppeler, Phys. Rev. D 89, 114012 (2014), arXiv:1404.2931 [hep-ph]

# Gaugino Annihilation

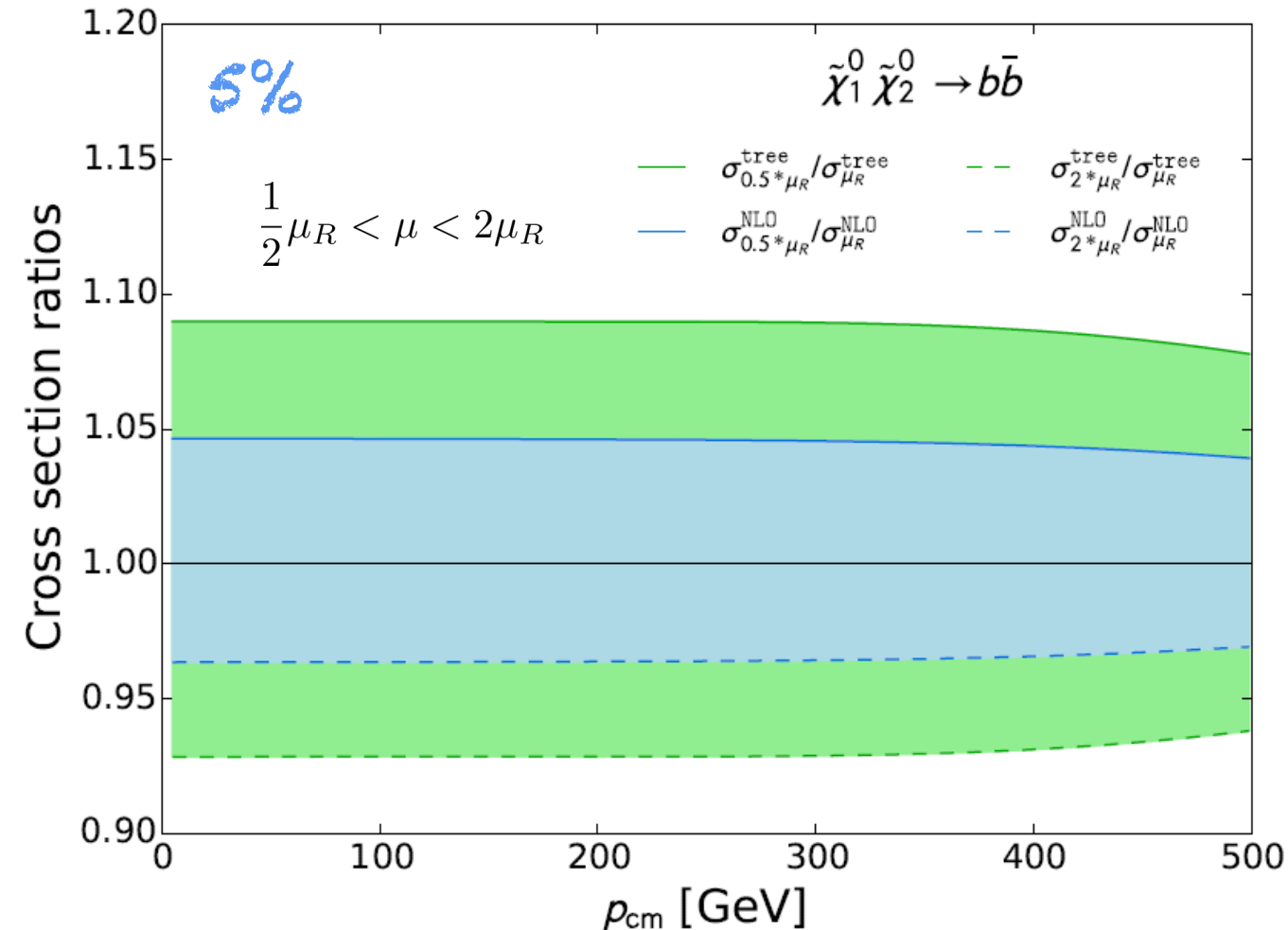
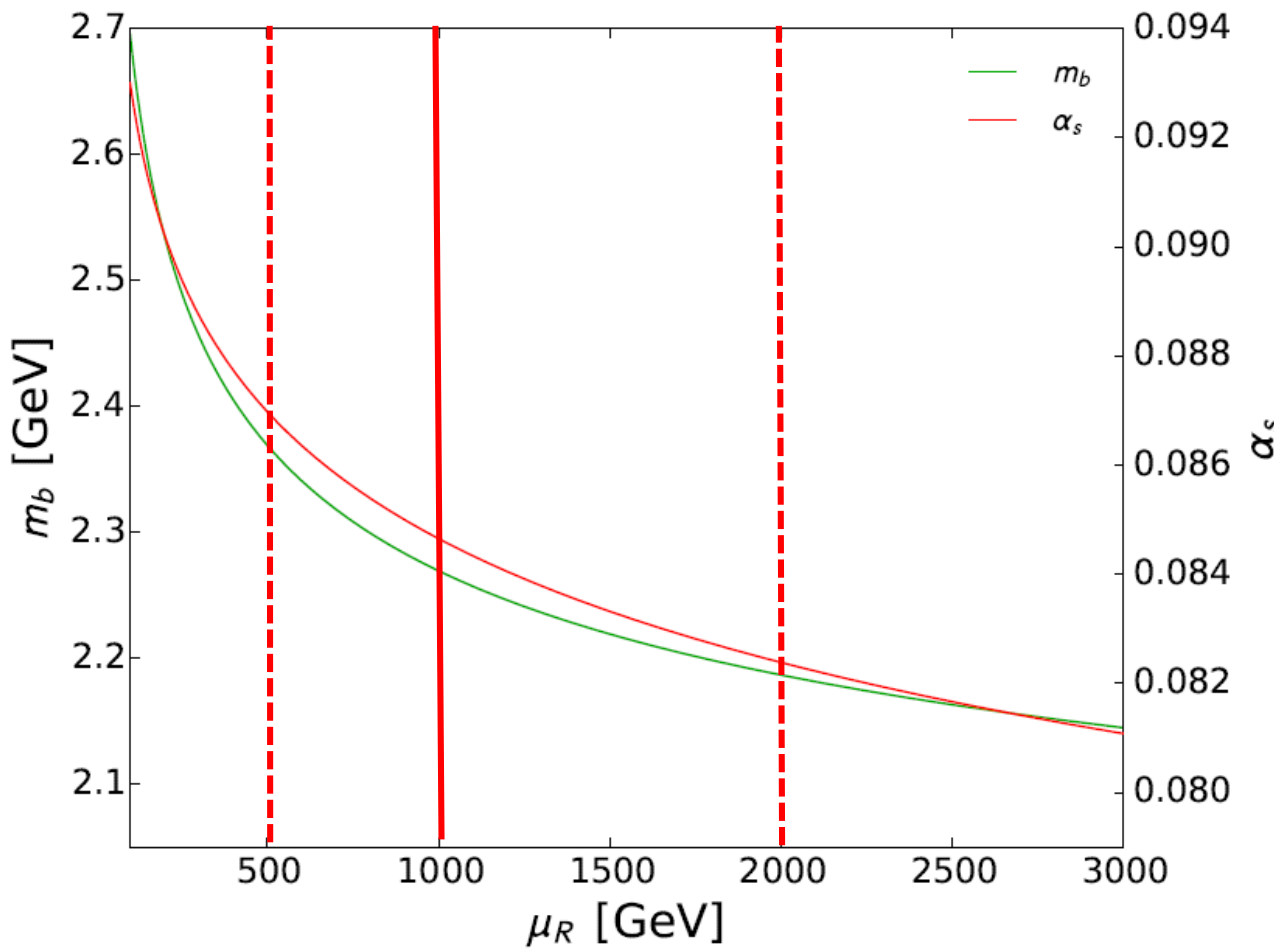


- NLO value does not lie within LO uncertainty band  $\leftarrow$  pure electroweak process
- **Larger** LO uncertainty band  $\leftarrow$  scale dependent  $m_b^{\overline{DR}}$
- **Smaller** NLO uncertainty band  $\leftarrow$  scale dependence decreased by virtual corrections to  $A^0 b\bar{b}$  coupling

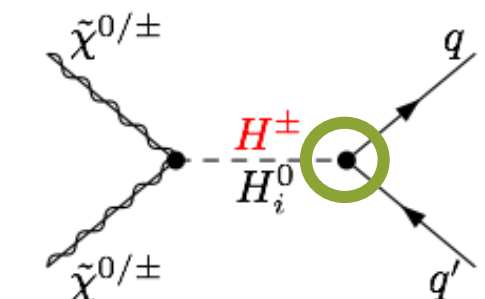
$\rightarrow$  NLO calculation shows 10-15% correction with respect to default MicrOMEGAs value  
 $\rightarrow$  5 % uncertainty on the NLO cross section



# Gaugino Annihilation

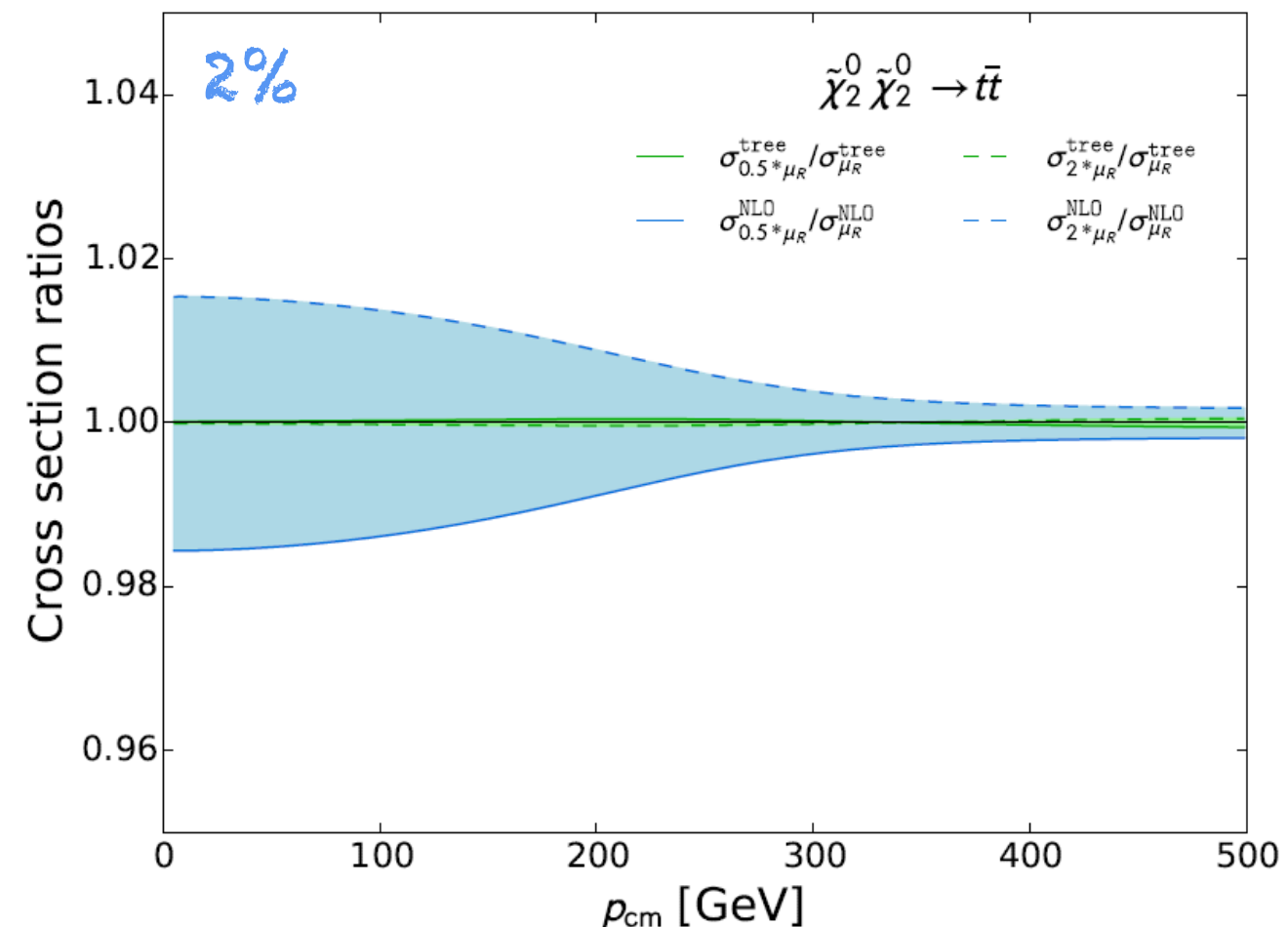
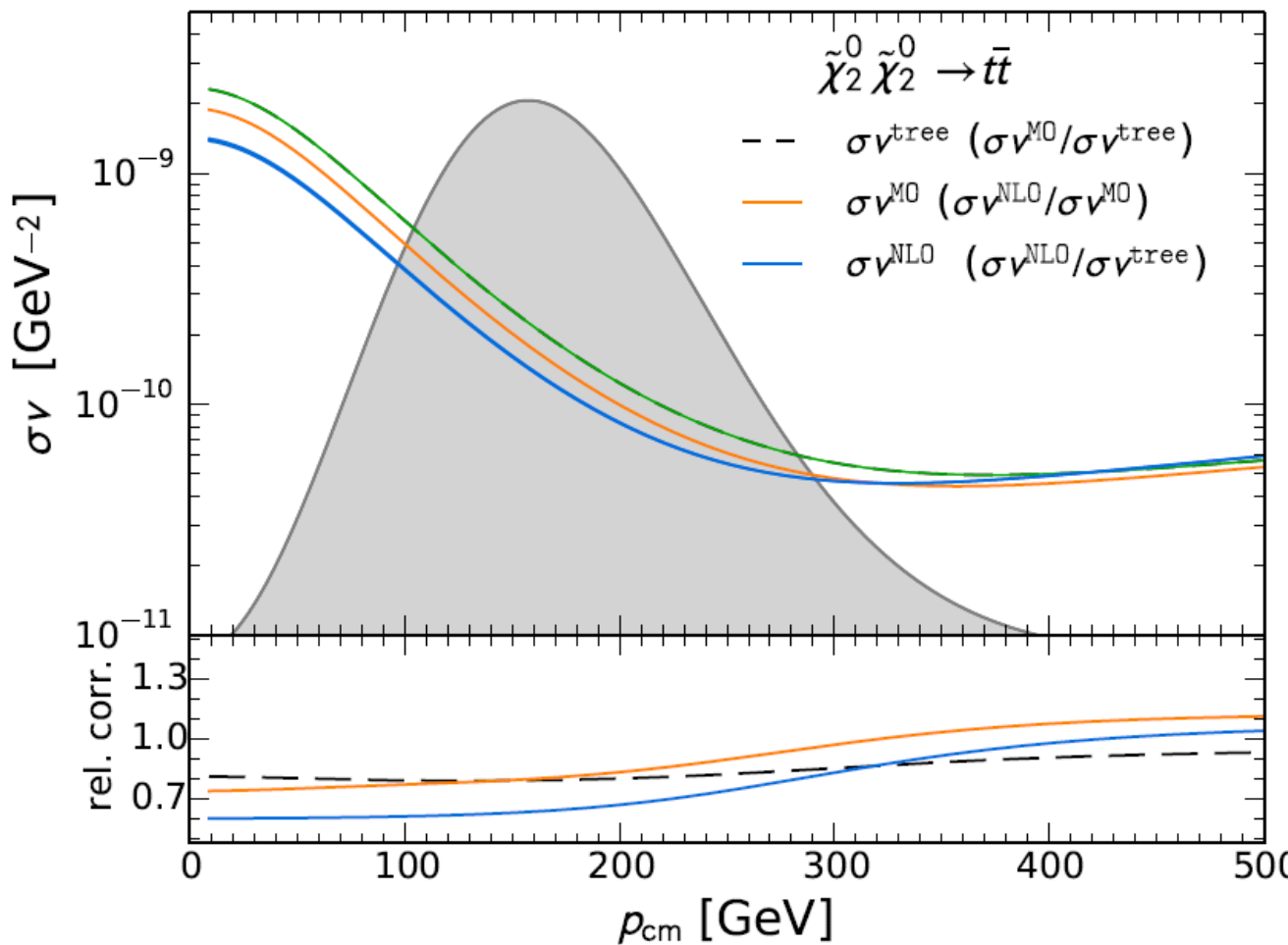


- NLO value does not lie within LO uncertainty band  $\leftarrow$  pure electroweak process
- **Larger** LO uncertainty band  $\leftarrow$  scale dependent  $m_b^{\overline{DR}}$
- **Smaller** NLO uncertainty band  $\leftarrow$  scale dependence decreased by virtual corrections to  $A^0 b\bar{b}$  coupling
  - $\rightarrow$  NLO calculation shows 10-15% correction with respect to default MicrOMEGAs value
  - $\rightarrow$  5 % uncertainty on the NLO cross section

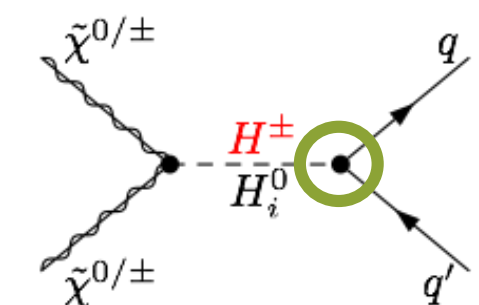


J. Harz, B. Herrmann, M. Klasen, K. Kovařík, and P. Steppeler, Phys. Rev. D 93 114023 (2016), arXiv:1602.08103 [hep-ph]  
 B. Herrmann, M. Klasen, K. Kovařík, M. Meinecke and P. Steppeler, Phys. Rev. D 89, 114012 (2014), arXiv:1404.2931 [hep-ph]

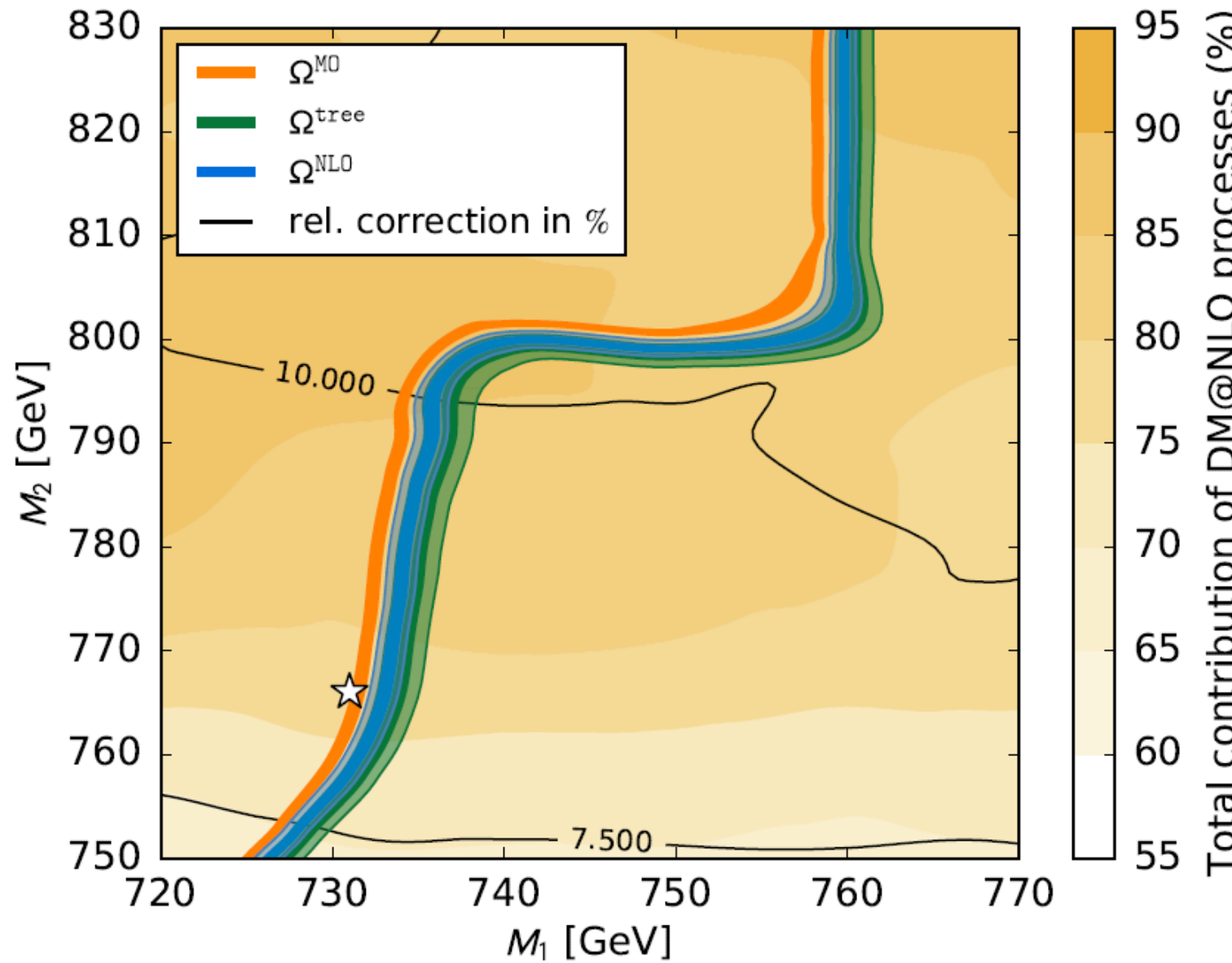
# Gaugino Annihilation



- Tiny scale dependence at LO and NLO
- **Smaller** LO uncertainty band  $\leftarrow$  scale independent  $m_t^{\text{OS}}$
- **Larger** NLO uncertainty band  $\leftarrow$  first appearance of scale dependent  $\alpha_s$ 
  - $\rightarrow$  size of theoretical uncertainty is process dependent
  - $\rightarrow$  theoretical uncertainty becomes possible to quantify only at NLO for the first time



# Gaugino Annihilation



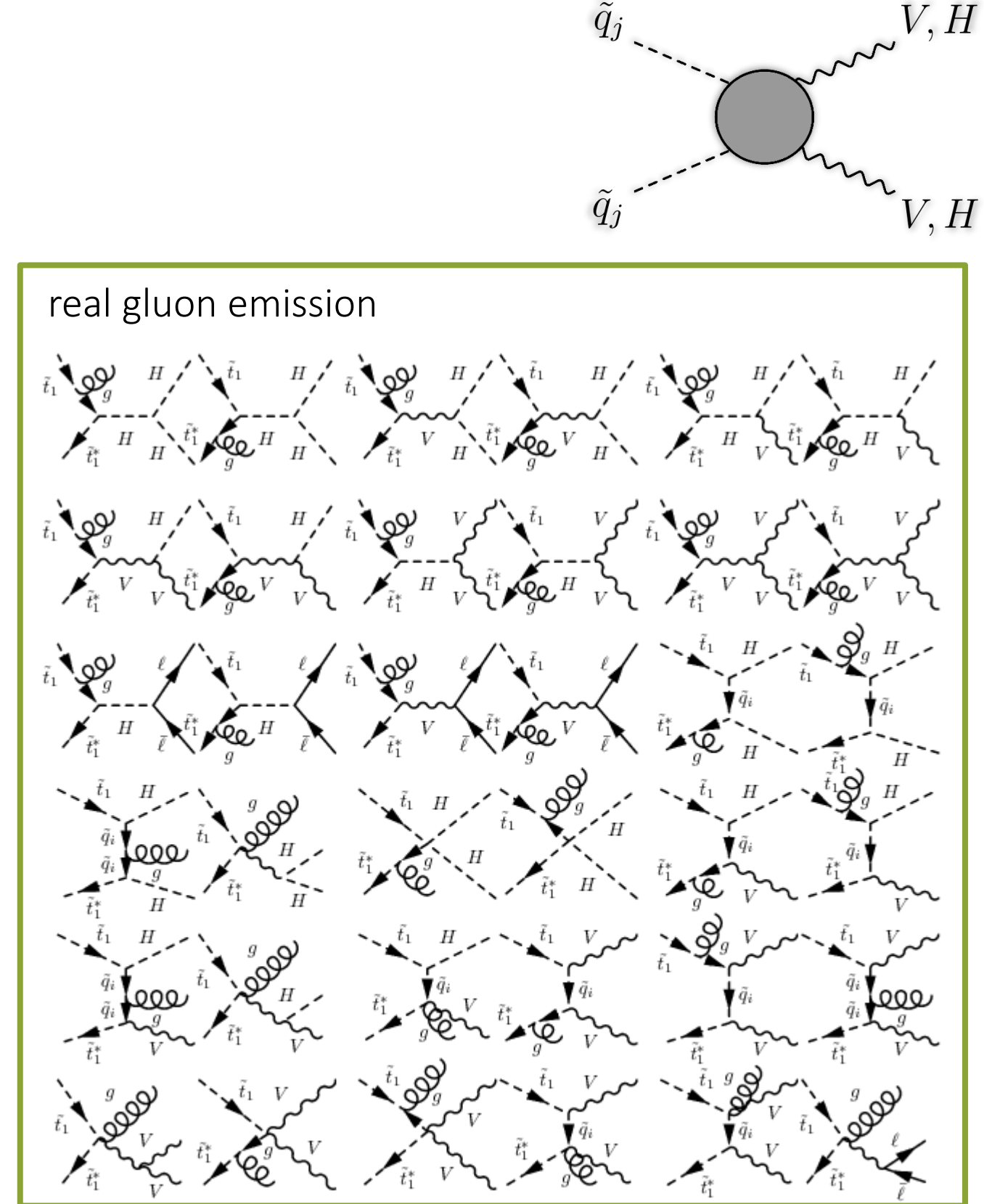
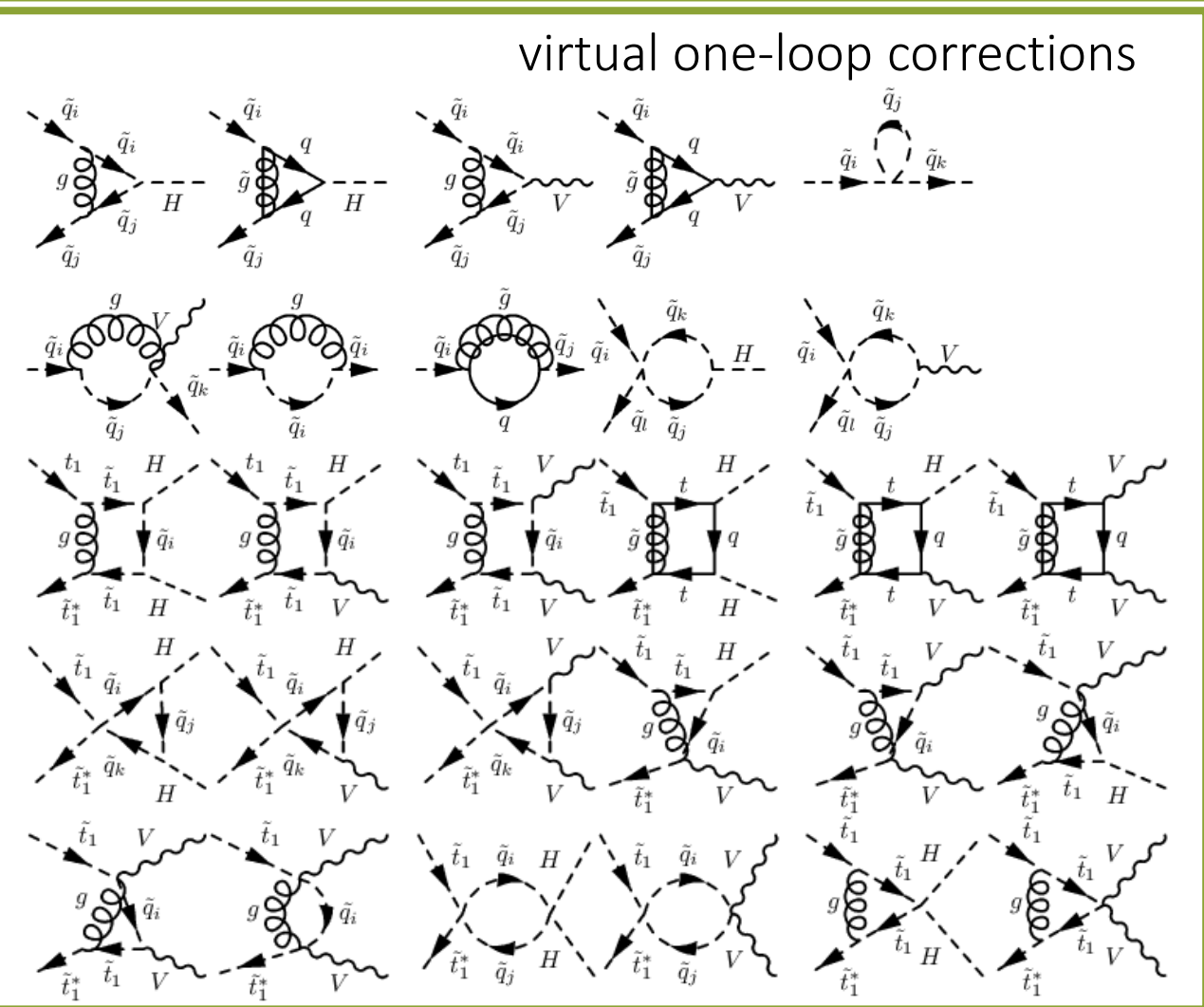
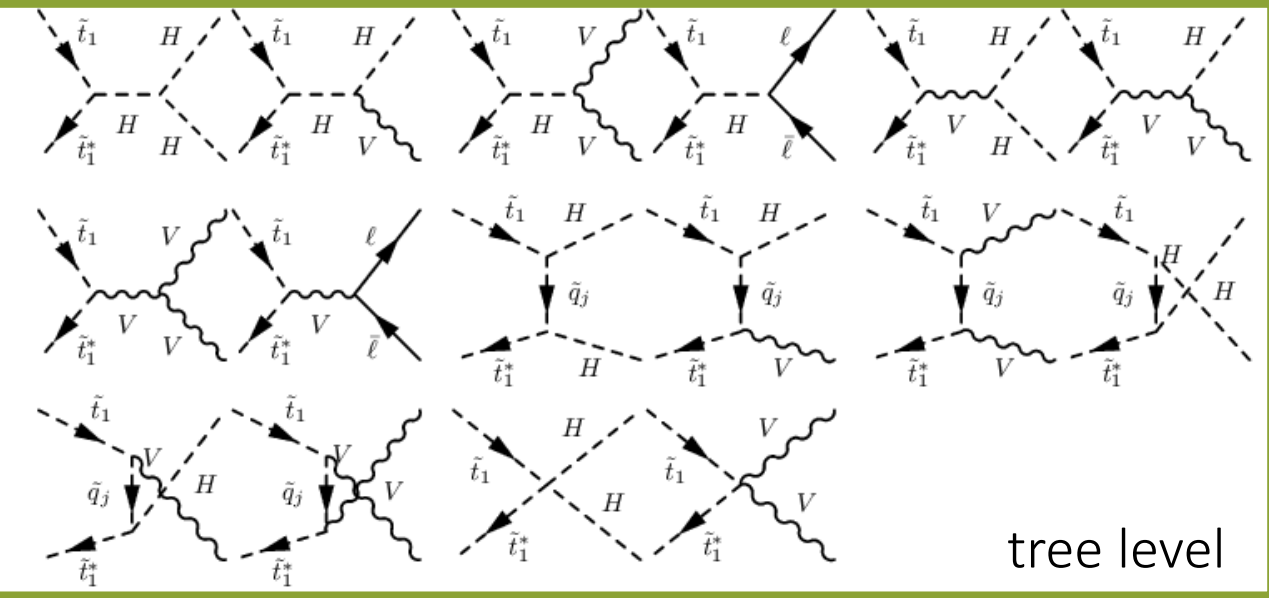
- scale dependence at LO mainly triggered by  $m_b^{\overline{DR}}$
- decreased scale dependence at NLO

- NLO calculation shows 5-10% relative correction with respect to default MO value
- shift in the parameter space with respect to MO value is larger than experimental uncertainty, even when including theoretical uncertainty
- error 2 times larger than naively expected

→ first quantitative estimation of theoretical uncertainty!

J. Harz, B. Herrmann, M. Klasen, K. Kovařík, and P. Steppeler, Phys.Rev. D 93 114023 (2016), arXiv:1602.08103 [hep-ph]

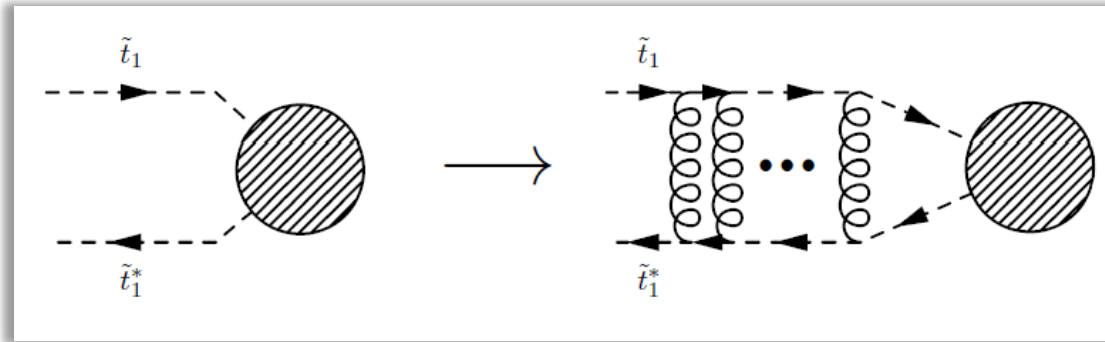
# Stop-Antistop Annihilation



J. Harz, B. Herrmann, M. Klasen, K. Kovařík, and M. Meinecke, Phys. Rev D 91 034012 (2015), arXiv:1410.8063 [hep-ph]

# Stop-Antistop Annihilation

+ Coulomb  
enhancement



- during freeze-out stop-antistop pair is moving slowly
- exchange of  $n$  gluons lead to a correction factor proportional to  $(\frac{\alpha_s}{v})^n$
- with  $\alpha_s/v > \mathcal{O}(1)$  Coulomb corrections can be become sizeable

→ resummation to all orders within framework of nonrelativistic QCD

M.J. Strassler and M.E.Peskin, Phys. Rev. D 43 1500 (1991)  
Y. Kiyo et al. Eur. Phys. J. C. 60 375 (2009)

# Stop-Antistop Annihilation

- Coulomb enhanced cross section factorises in LO cross section and Greens function:

$$\sigma^{\text{Coul.}}(\tilde{t}_1 \tilde{t}_1^* \rightarrow \text{EW}) = \frac{4\pi}{vm_{\tilde{t}_1}^2} \Im \left\{ G^{[1]}(\mathbf{r} = 0; \sqrt{s} + i\Gamma_{\tilde{t}_1}, \mu_C) \right\} \times \sigma^{\text{LO}}(\tilde{t}_1 \tilde{t}_1^* \rightarrow \text{EW})$$

- Greens function is determined as solution of the would-be stoponium Schrödinger equation

$$[H^{[1]} - (\sqrt{s} + i\Gamma_{\tilde{t}_1})]G^{[1]}(\mathbf{r}; \sqrt{s} + i\Gamma_{\tilde{t}_1}, \mu_C) = \delta^{(3)}(\mathbf{r})$$

M.J. Strassler and M.E. Peskin, Phys. Rev. D 43 1500 (1991)

Y. Kiyo et al. Eur. Phys. J. C. 60 375 (2009)

$$H^{[1]} = -\frac{1}{m_{\tilde{t}_1}}\Delta + 2m_{\tilde{t}_1} + V^{[1]}(\mathbf{r}) \quad \tilde{V}^{[1]}(\mathbf{q}) = -\frac{4\pi\alpha_s(\mu_C)C^{[1]}}{\mathbf{q}^2} \times \left[ 1 + \frac{\alpha_s(\mu_C)}{4\pi} \left( \beta_0 \ln \frac{\mu_C^2}{\mathbf{q}^2} + a_1 \right) \right]$$

Coulomb potential  
@ NLO  $\mathcal{O}((\alpha_s^2/v)^n)$

- Greens function carries scale as it has to be regularised at  $r = 0$
- Scale is independent of renormalisation scale, chosen to be close to inverse Bohr radius (characteristic scale of stoponium bound state)
- Explicit logarithmic scale dependence kicks in only at NNLO:

$$\Im \left\{ G^{[1]}(0; \sqrt{s} + i\Gamma_{\tilde{t}_1}, \mu_C) \right\} = m_{\tilde{t}_1}^2 \Im \left\{ \frac{v}{4\pi} \left[ i + \frac{\alpha_s(\mu_C)C_F}{v} \left( \frac{i\pi}{2} + \ln \frac{\mu_C}{2m_{\tilde{t}_1}v} \right) + \mathcal{O}(\alpha_s^2) \right] \right\}$$

→ In the following: vary Coulomb scale as well around its central value

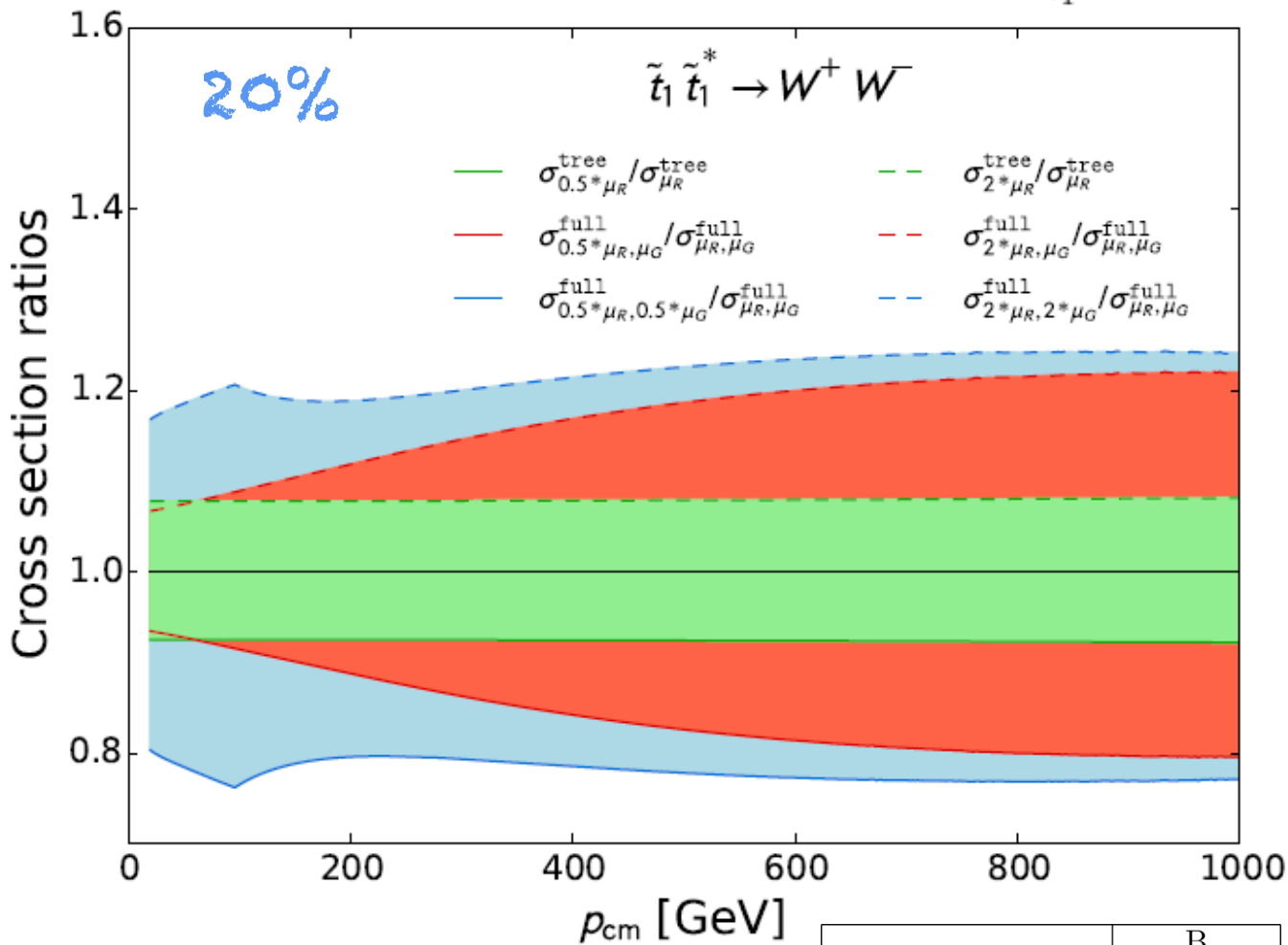
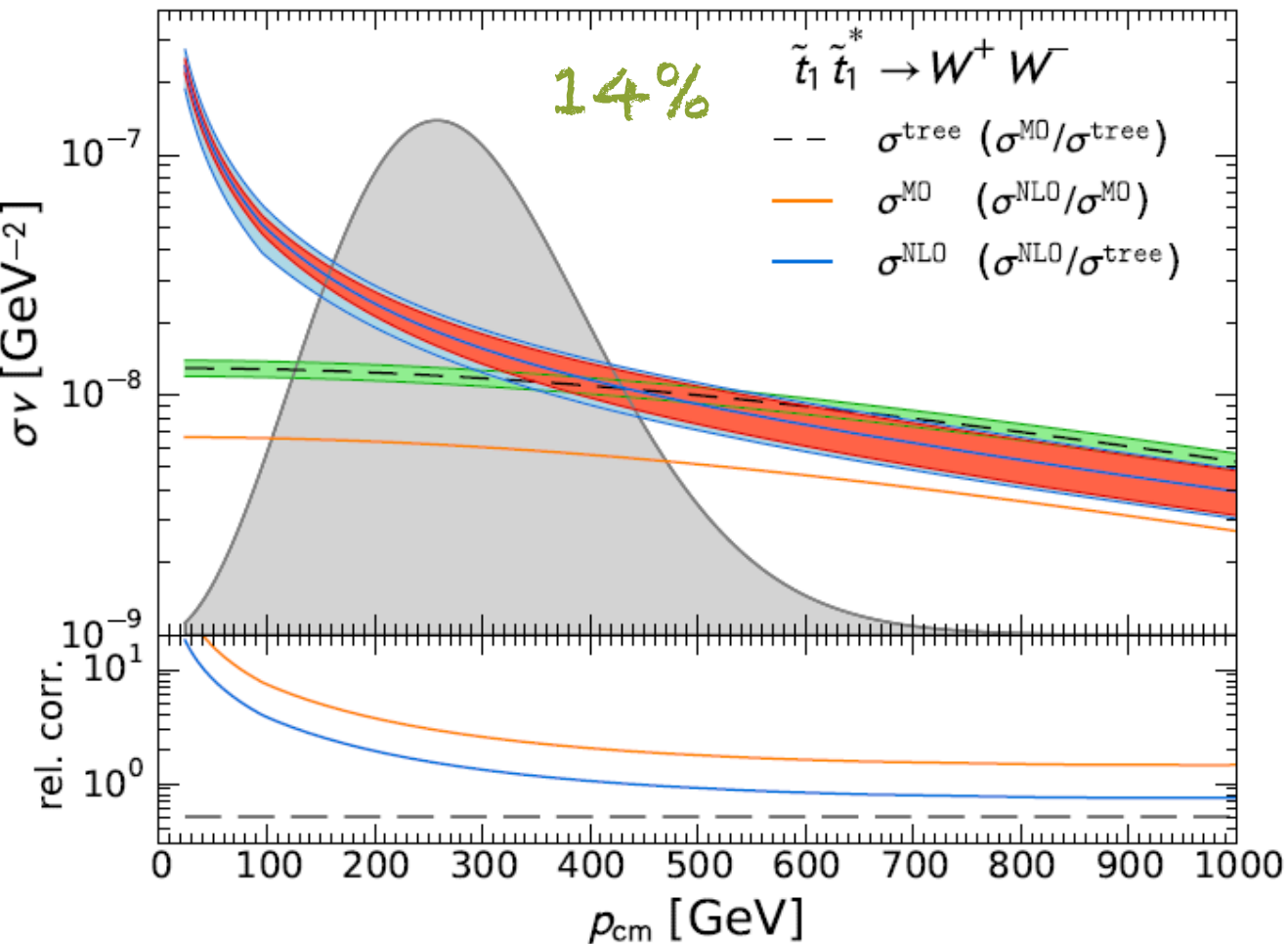
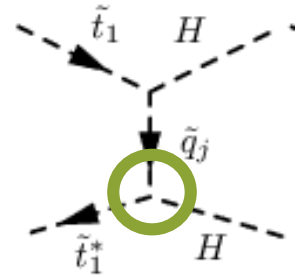
$$\frac{1}{2}\mu_C < \mu < 2\mu_C$$

J. Harz, B. Herrmann, M. Klasen, K. Kovařík, and M. Meinecke, Phys. Rev D 91 034012 (2015), arXiv:1410.8063 [hep-ph]

# Stop-Antistop Annihilation

Scenario with a small mass gap between LSP and NLSP

	$m_{\tilde{\chi}_1^0}$	$m_{\tilde{\chi}_2^0}$	$m_{\tilde{\chi}_1^\pm}$	$m_{\tilde{\chi}_2^\pm}$	$m_{\tilde{t}_1}$	$m_{\tilde{t}_2}$	$Z_{1\tilde{B}}$	$Z_{1\tilde{W}}$	$Z_{1\tilde{H}_1}$	$Z_{1\tilde{H}_2}$	$m_{h^0}$	$\Omega_{\tilde{\chi}_1^0} h^2$	$\text{BR}(b \rightarrow s\gamma)$
B	1306.3	1827.0	1827.2	2640.0	1361.7	2157.3	-1.000	0.002	-0.024	0.013	123.7	0.1134	$3.1 \cdot 10^{-4}$

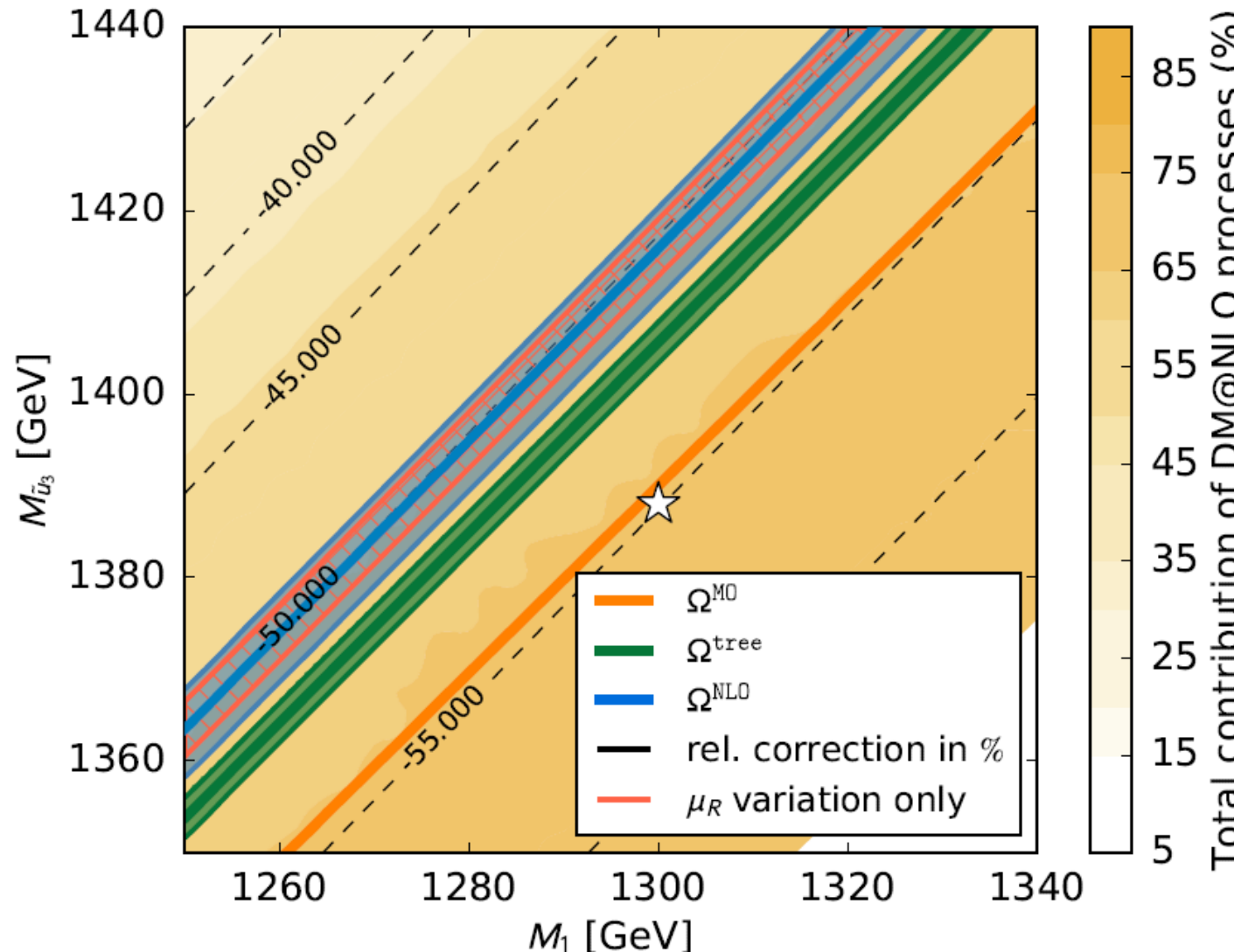


- Scale dependence at LO triggered by trilinear coupling  $A_t$
  - Scale dependence at NLO due to explicit logarithms and implicit ( $A_t \alpha_s$ )
  - Coulomb-scale leads to 20% uncertainty
- large correction (K-factor of 1-9) in relevant region, 20 % theoretical error

	B
$\tilde{\chi}_1^0 \tilde{t}_1 \rightarrow th^0$	1%
$\tilde{\chi}_1^0 \tilde{t}_1 \rightarrow tg$	6%
$\tilde{t}_1 \tilde{t}_1^* \rightarrow h^0 h^0$	12%
$\tilde{t}_1 \tilde{t}_1^* \rightarrow h^0 H^0$	11%
$\tilde{t}_1 \tilde{t}_1^* \rightarrow Z^0 A^0$	7%
$\tilde{t}_1 \tilde{t}_1^* \rightarrow W^\pm H^\mp$	13%
$\tilde{t}_1 \tilde{t}_1^* \rightarrow Z^0 Z^0$	8%
$\tilde{t}_1 \tilde{t}_1^* \rightarrow W^+ W^-$	14%
Total	72%

# Stop-Antistop Annihilation

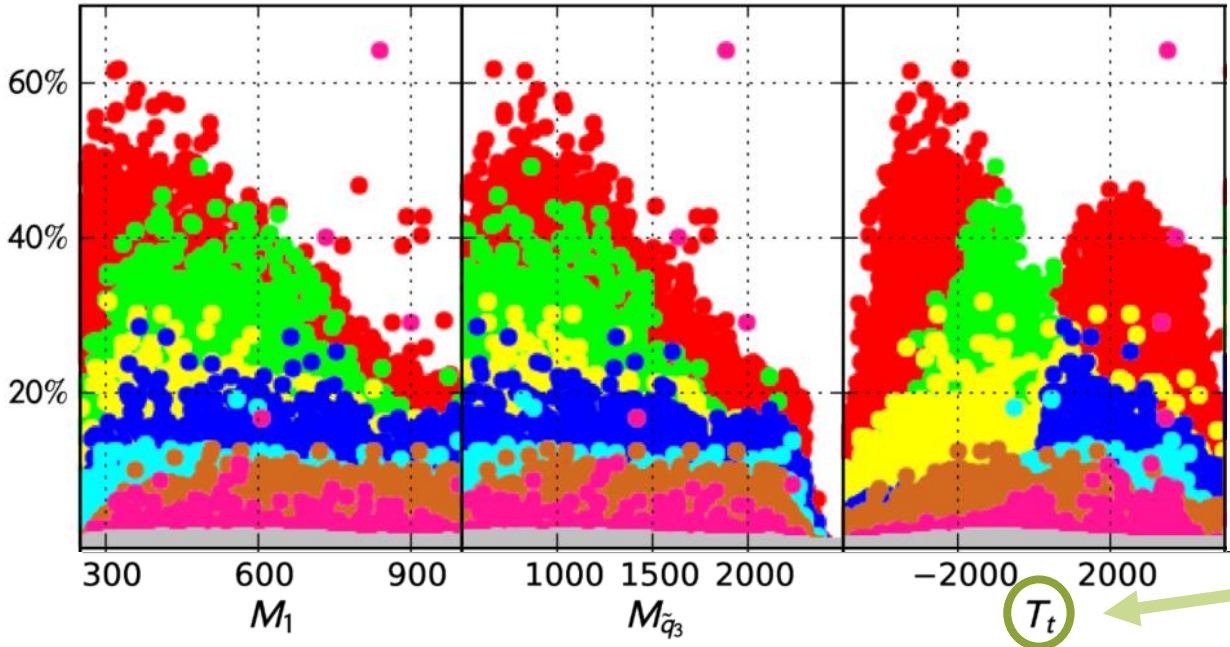
Scenario with a small mass gap between LSP and NLSP



	B
$\tilde{\chi}_1^0 \tilde{t}_1 \rightarrow th^0$	1%
$\tilde{t}_1 g$	6%
$\tilde{t}_1 \tilde{t}_1^* \rightarrow h^0 h^0$	12%
$h^0 H^0$	11%
$Z^0 A^0$	7%
$W^\pm H^\mp$	13%
$Z^0 Z^0$	8%
$W^+ W^-$	14%
Total	72%

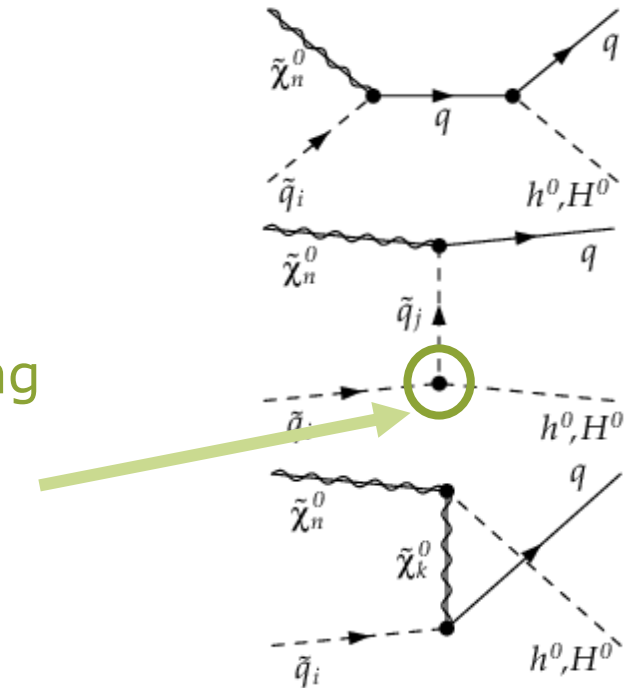
- NLO calculation shows 50-60% relative difference with respect to default MO value
- even including theoretical uncertainty, significant shift in the parameter space with respect to the MO value
- mass shift of 30 GeV with an accuracy of 0.5%
- error 5 times larger than naively expected

# Stop Coannihilation



$$\begin{aligned}\tilde{\chi} \tilde{t} &\rightarrow th^0 \\ \tilde{\chi} \tilde{t} &\rightarrow tg \\ \tilde{\chi} \tilde{t} &\rightarrow tZ^0\end{aligned}$$

large trilinear coupling  
enhances  $\tilde{\chi}_1^0 \tilde{t}_1 \rightarrow th$   
via t-channel stop-  
exchange



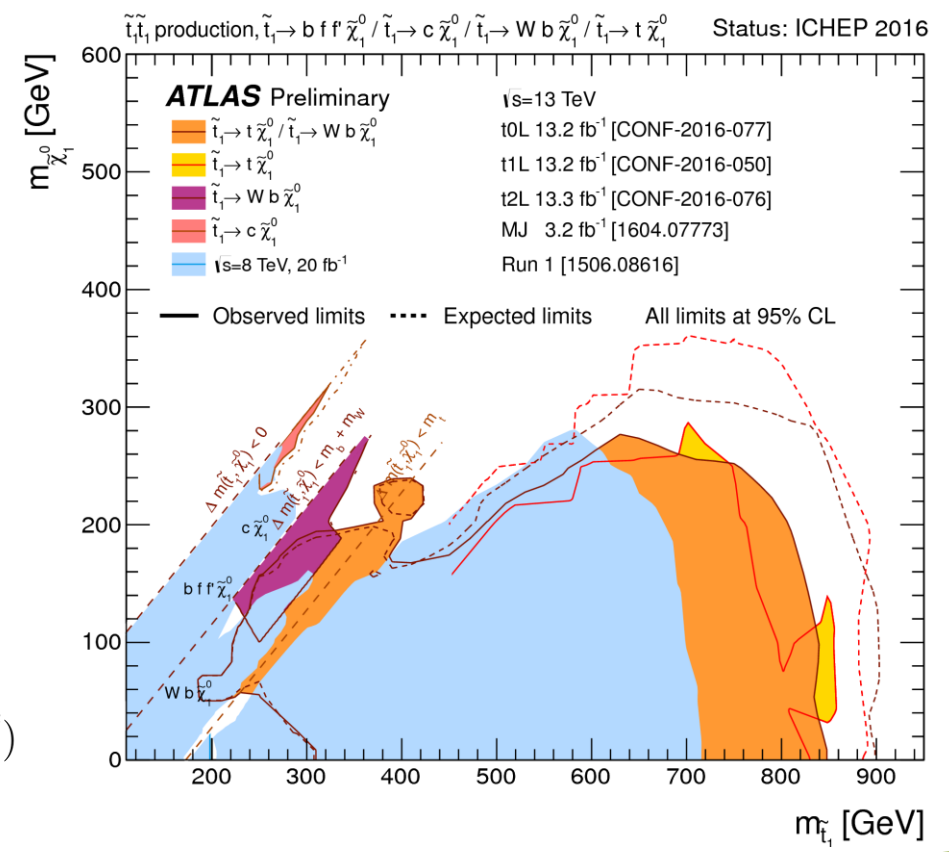
observed Higgs mass of 125 GeV suggests large stop mass splitting, e.g. triggered by large trilinear coupling At

$$m_{h_0}^2 \approx m_Z^2 \cos^2 2\beta + \frac{3g^2 m_t^4}{8\pi^2 m_W^2} \left[ \ln \frac{M_{\text{SUSY}}^2}{m_t^2} + \frac{X_t^2}{M_{\text{SUSY}}^2} \left( 1 - \frac{X_t^2}{12 M_{\text{SUSY}}^2} \right) \right]$$

$$X_t = A_t - \mu / \tan \beta$$

$$M_{\text{SUSY}} = \sqrt{m_{\tilde{t}_1} m_{\tilde{t}_2}}$$

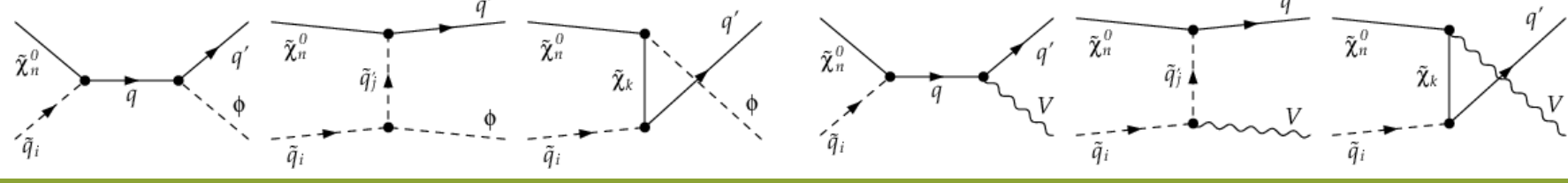
$$\begin{pmatrix} m_{\tilde{t}_1}^2 & 0 \\ 0 & m_{\tilde{t}_2}^2 \end{pmatrix} = U^{\tilde{q}} \begin{pmatrix} M_{\tilde{Q}}^2 + m_t^2 + (I_q^{3L} - e_q \sin_W^2) \cos 2\beta m_Z^2 \\ m_t X_t \\ M_{\tilde{U}}^2 + m_t^2 + e_q \sin_W^2 \cos 2\beta m_Z^2 \end{pmatrix} (U^{\tilde{q}})$$



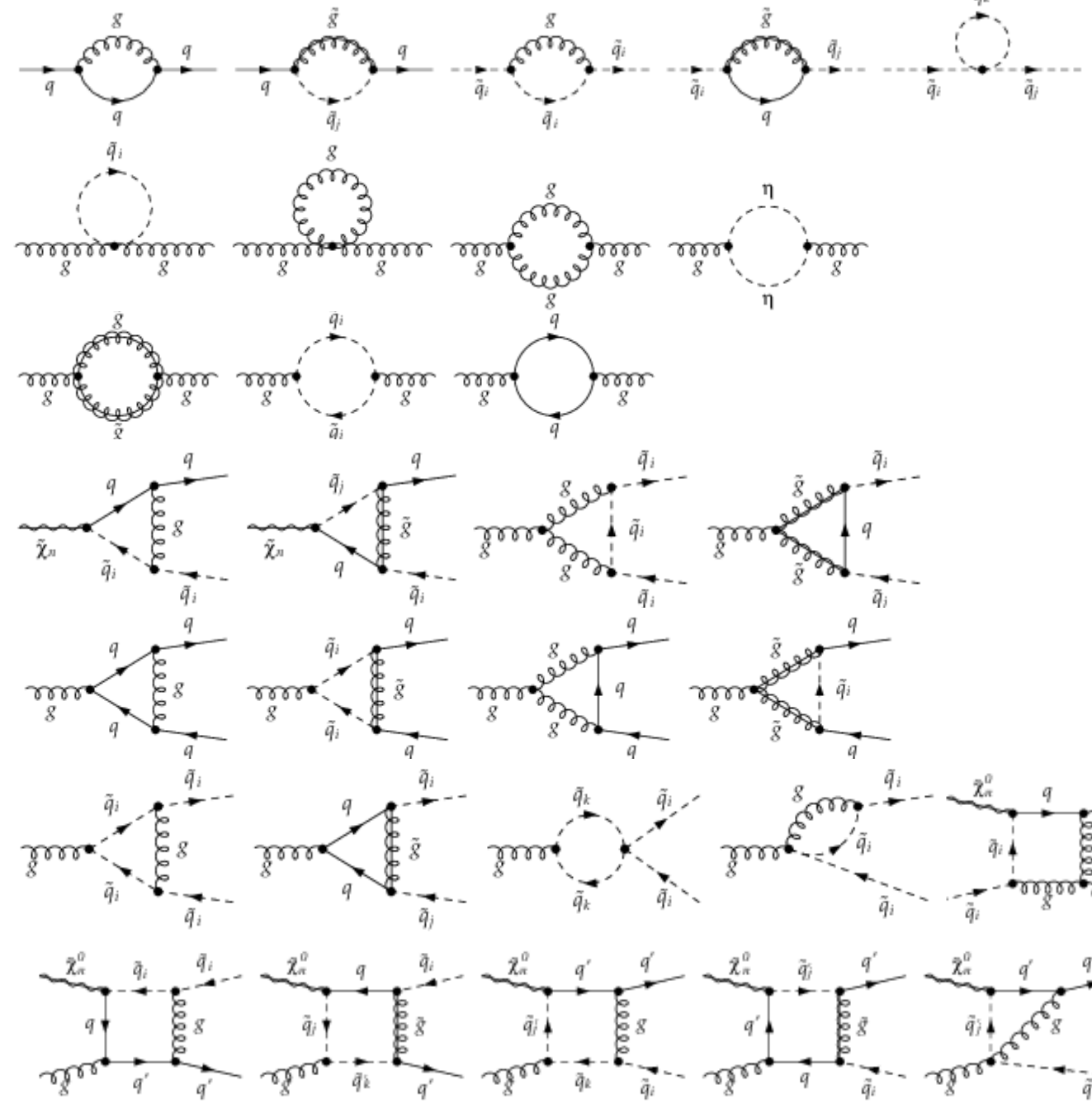
J. Harz, B. Herrmann, M. Klasen, K. Kovařík and Q. Le Bouc'h, Phys. Rev. D 87, 054031 (2013), arXiv:1212.5241 [hep-ph]

# Stop Coannihilation

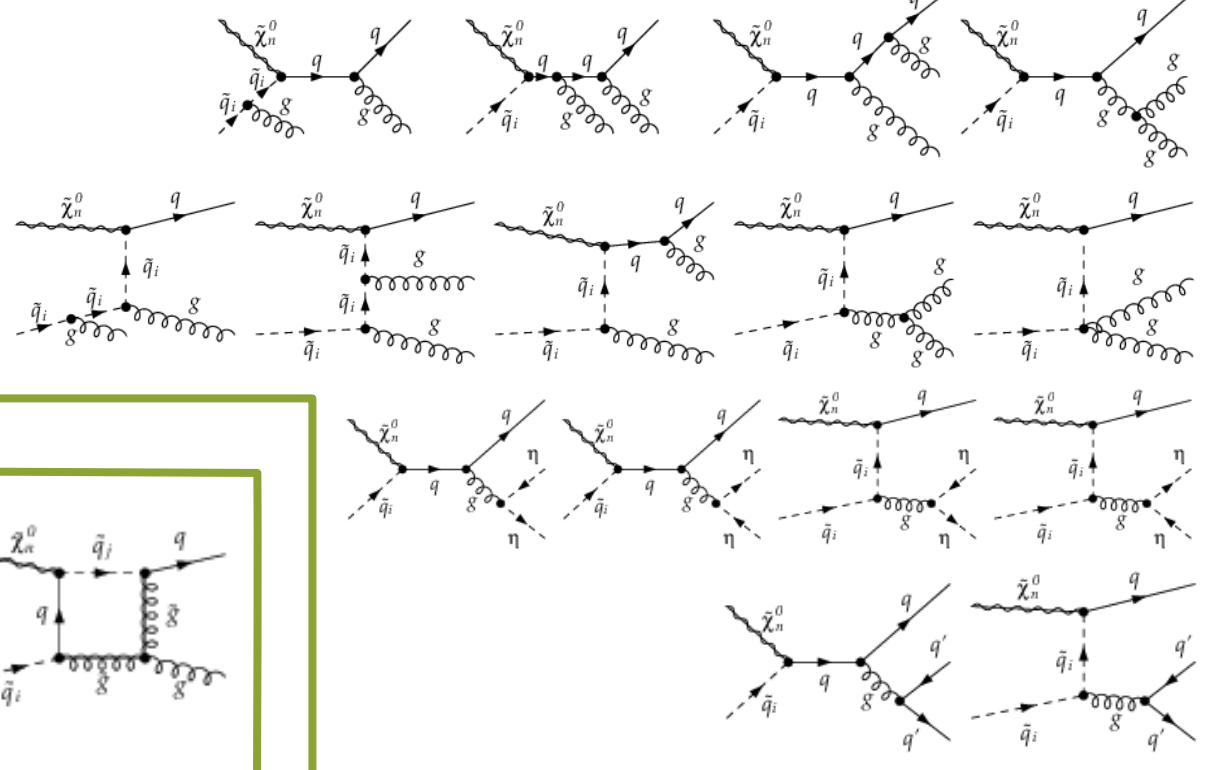
Tree level



Virtual one-loop corrections

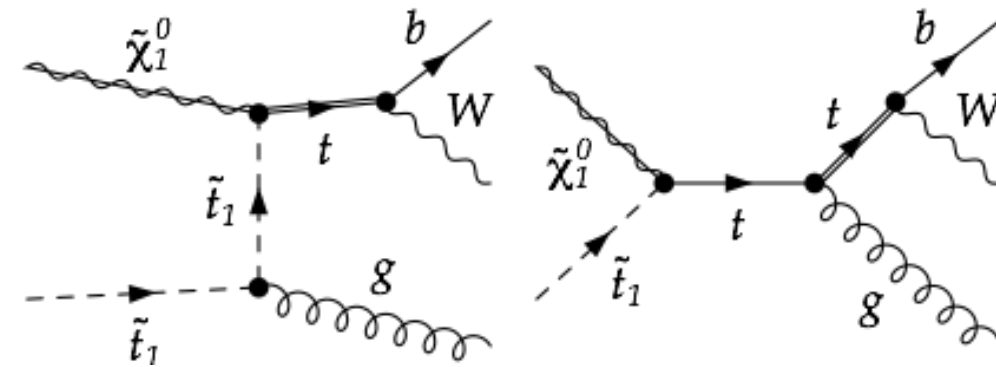


Real gluon emission processes



# Stop Coannihilation – intermediate OS states

- with  $m_t > m_b + m_W$  an intermediate on-shell state can occur as soon as  $\sqrt{s} > m_t$



- local on-shell subtraction (DS) / "Prospino" scheme

W. Beenakker, R. Hoepker, M. Spira, P.M. Zerwas, Nuclear Physics B 492 (1997)

$$|\mathcal{M}|^2 = |\mathcal{M}_{\text{res}}|^2 - |\mathcal{M}_{\text{res}}^{\text{sub}}|^2 + 2\text{Re}(\mathcal{M}_{\text{res}}^* \mathcal{M}_{\text{rem}}) + |\mathcal{M}_{\text{rem}}|^2$$

- "counterterm" consists of Breit-Wigner weighted on-shell squared matrix element

$$|\mathcal{M}_{\text{res}}^{\text{sub}}|^2 = \frac{m_t^2 \Gamma_t^2}{(p_t^2 - m_t^2)^2 + m_t^2 \Gamma_t^2} |\mathcal{M}_{\text{res}}|_{p_t^2 = m_t^2}^2$$

- resonant propagators are regularized by Breit-Wigner propagator

→ consistent, width independent, gauge invariant treatment retaining interference terms

# Combined Scenario incl. Stop Coannihilation

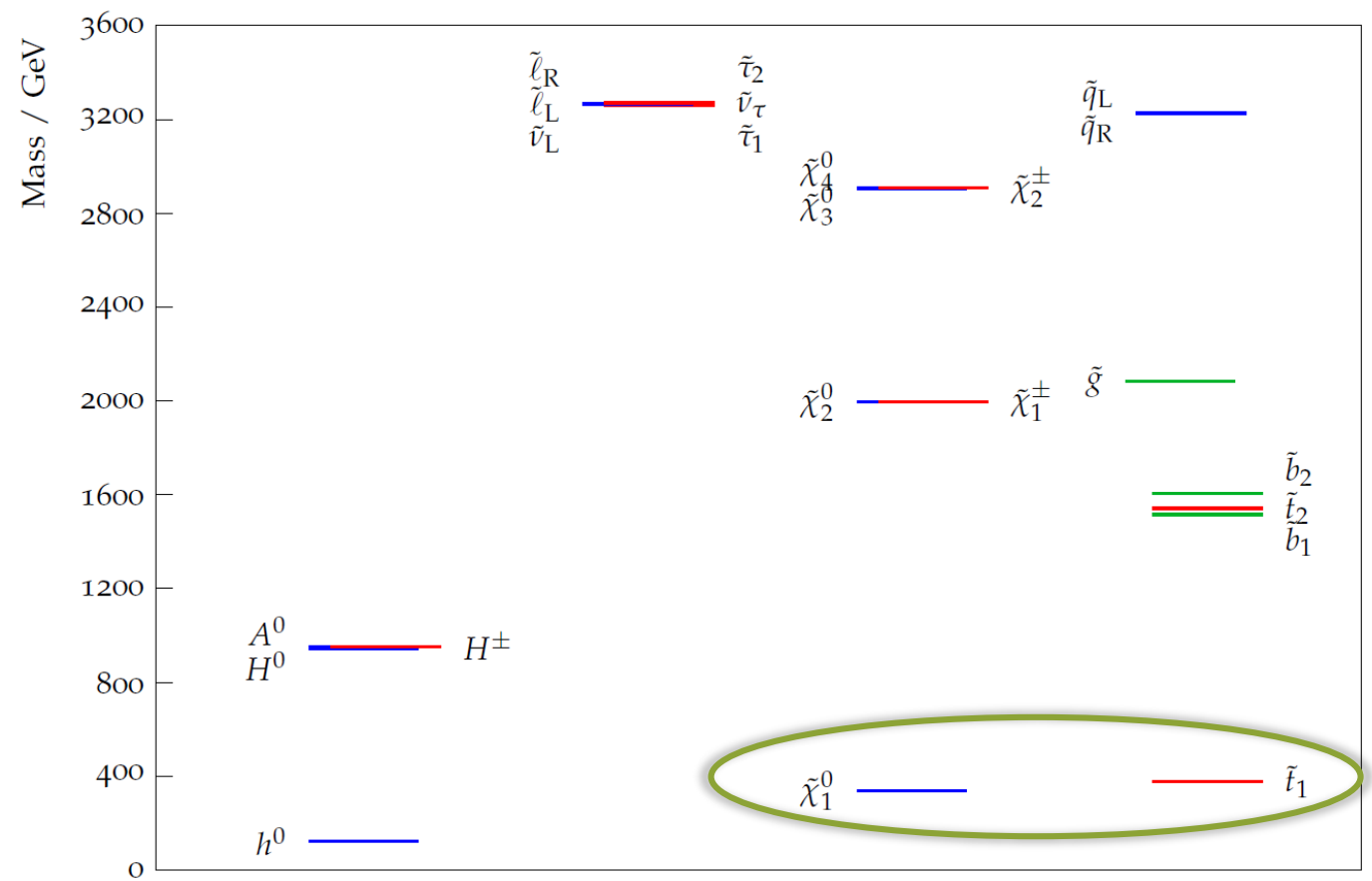
## Combined scenario features

- gaugino annihilation
- Neutralino-Stop Coannihilation
- Stop-Antistop-Anhilation

$\tan \beta$	$\mu$	$m_A$	$M_1$	$M_2$	$M_3$	$M_{\tilde{q}_{1,2}}$	$M_{\tilde{q}_3}$	$M_{\tilde{u}_3}$	$M_{\tilde{\ell}}$	$T_t$	Input parameter
5.8	2925.8	948.8	335.0	1954.1	1945.6	3215.1	1578.0	609.2	3263.9	2704.1	pMSSM11

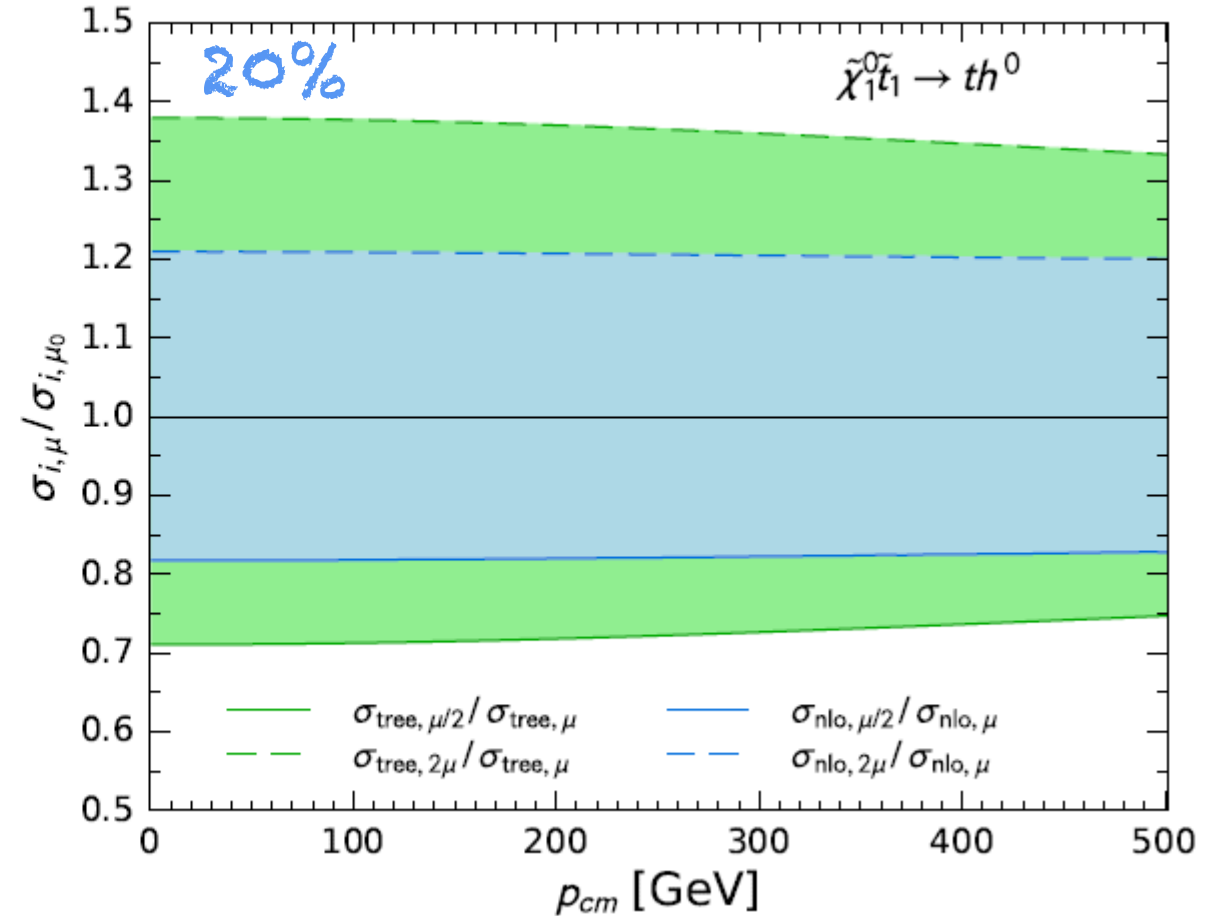
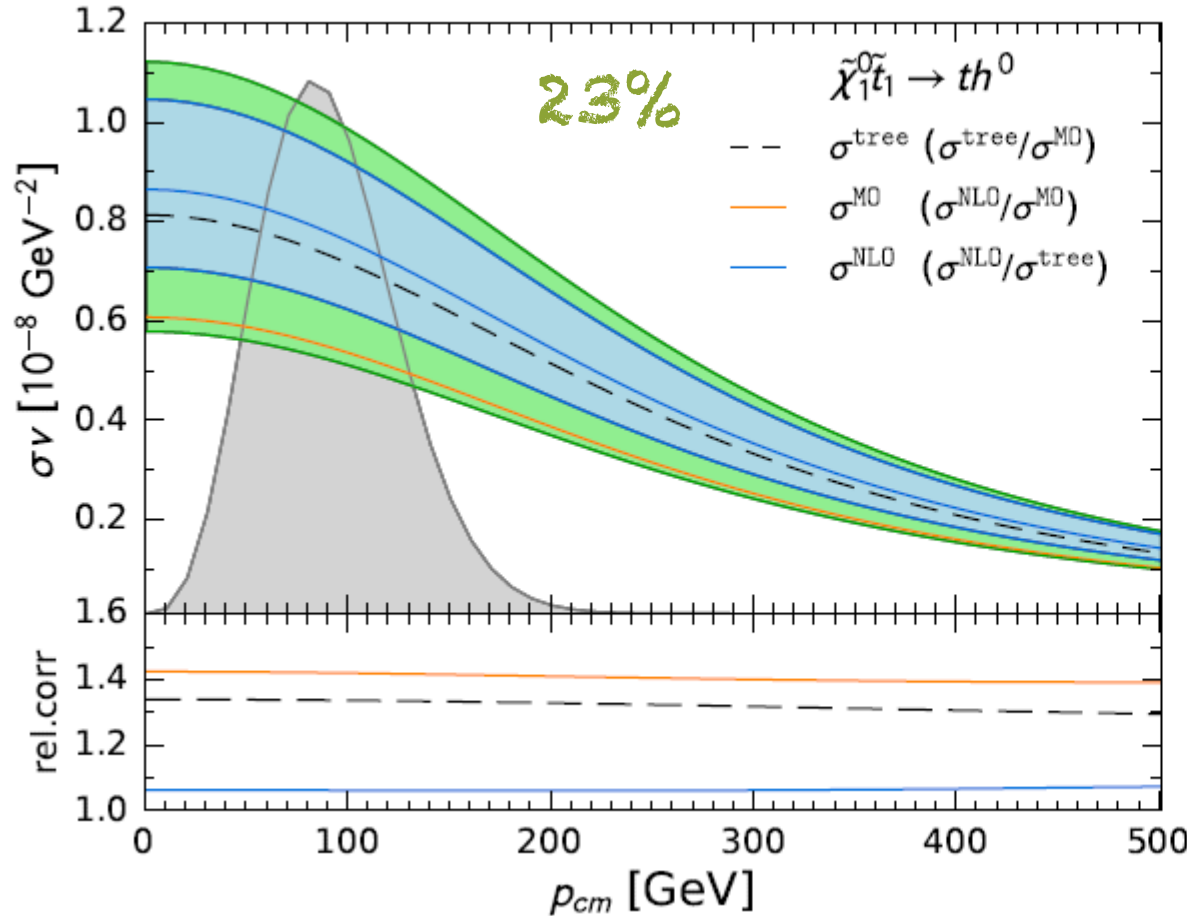
$m_{\tilde{\chi}_1^0}$	$m_{\tilde{t}_1}$	$m_{\tilde{h}^0}$	$\Omega_{\tilde{\chi}_1^0} h^2$	$\text{BR}(b \rightarrow s\gamma)$	Masses & observables
338.3GeV	375.6GeV	122.0GeV	0.1135	$3.25 \cdot 10^{-4}$	

	C
$\tilde{\chi}_1^0 \tilde{\chi}_1^0 \rightarrow t\bar{t}$	16%
$\tilde{\chi}_1^0 \tilde{t}_1 \rightarrow th^0$	23%
$tg$	23%
$tZ^0$	5%
$bW^+$	11%
$\tilde{t}_1 \tilde{t}_1^* \rightarrow h^0 h^0$	5%
$Z^0 Z^0$	2%
$W^+ W^-$	3%
Total	88%

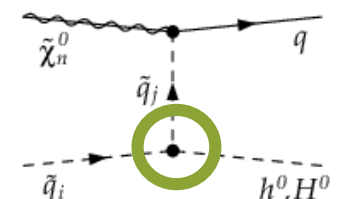


J. Harz, B. Herrmann, M. Klasen, K. Kovařík and Q. Le Bouc'h, Phys. Rev. D 87, 054031 (2013), arXiv:1212.5241 [hep-ph]  
 J. Harz, B. Herrmann, M. Klasen, and K. Kovařík, Phys. Rev. D 91, 034028 (2015), arXiv:1409.2898 [hep-ph]

# Stop Coannihilation



- Scale dependence at LO triggered by trilinear coupling  $A_t$
- Scale dependence at NLO due to explicit logarithms and implicit  $A_t$   $\alpha_s$
- Scale uncertainty of 20%

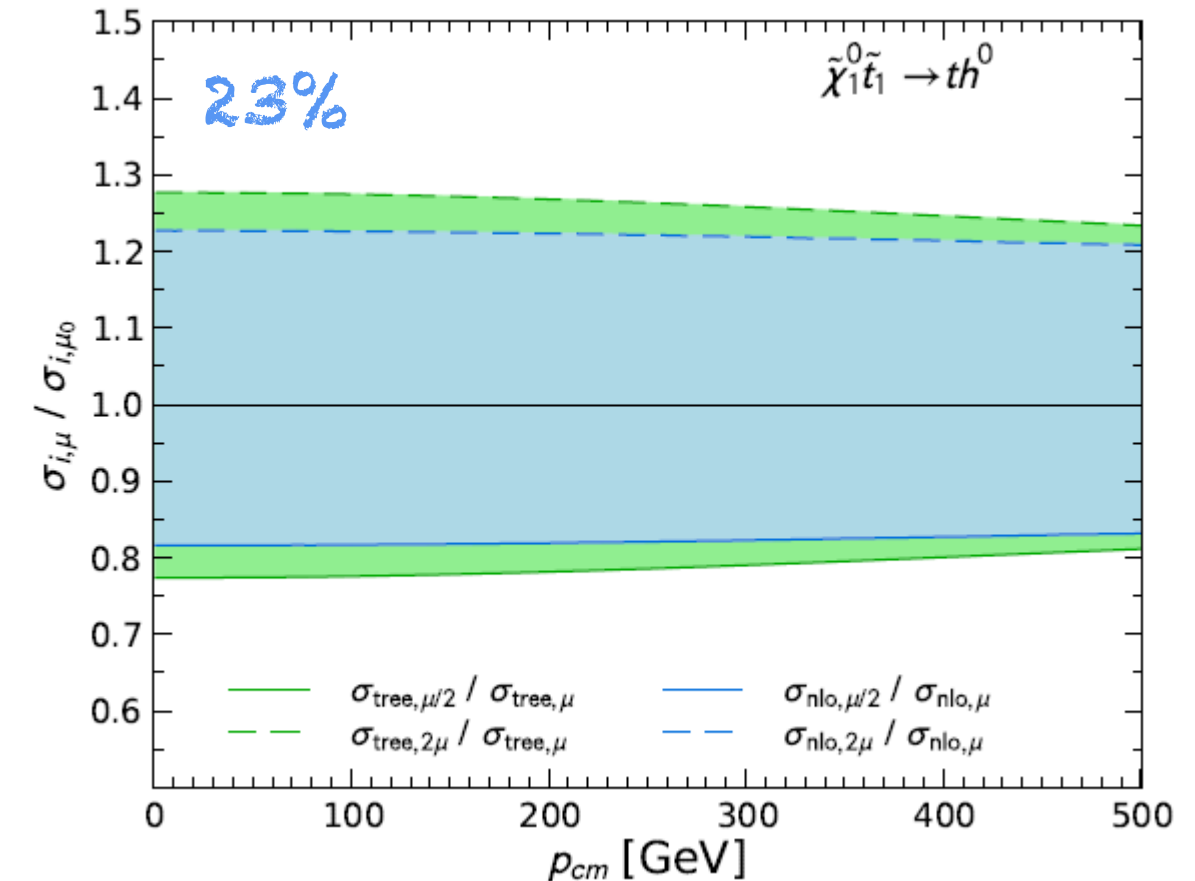
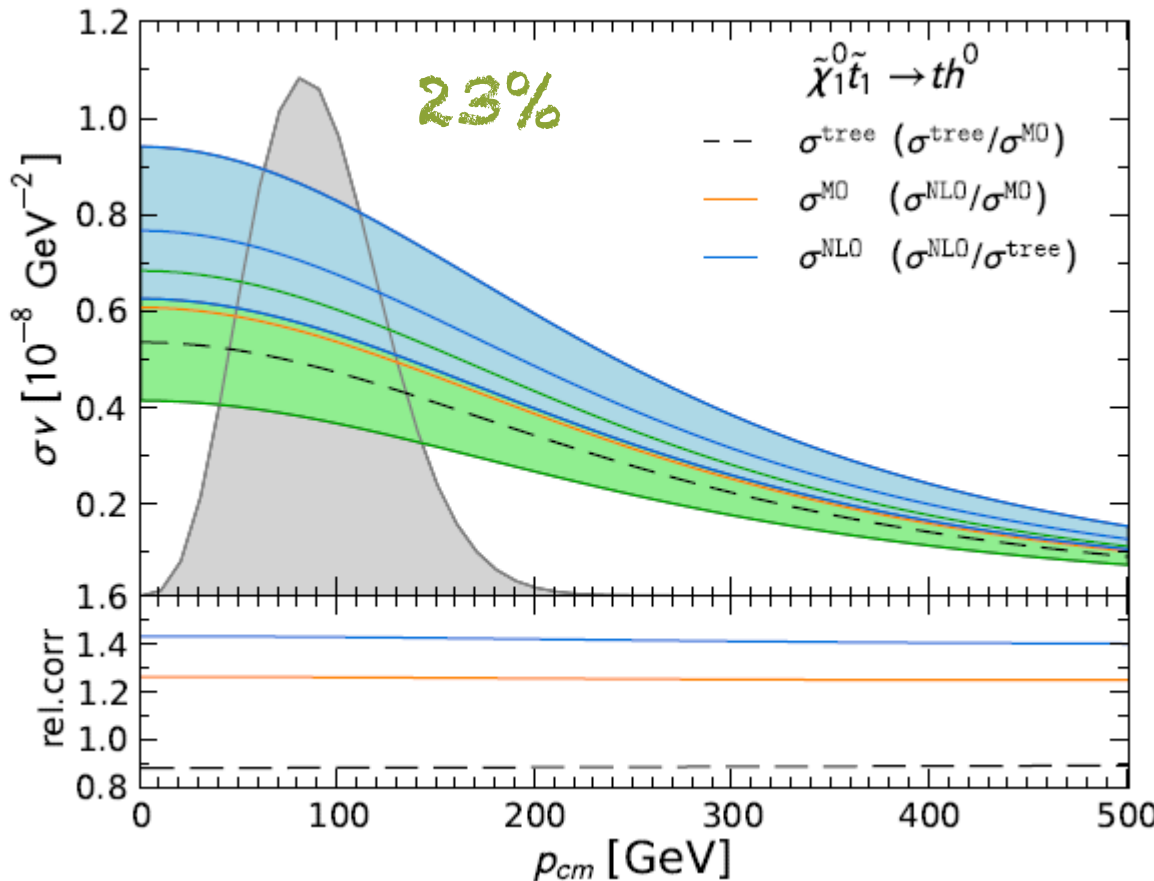


→ K-factor of 1.05, correction of 40% w.r.t. MicrOMEGAs, 20 % theoretical uncertainty

J. Harz, B. Herrmann, M. Klasen, K. Kovařík, and P. Steppeler, Phys. Rev. D 93 114023 (2016), arXiv:1602.08103 [hep-ph]  
 J. Harz, B. Herrmann, M. Klasen, and K. Kovařík, Phys. Rev. D 91, 034028 (2015), arXiv:1409.2898 [hep-ph]  
 J. Harz, B. Herrmann, M. Klasen, K. Kovařík and Q. Le Bouc'h, Phys. Rev. D 87, 054031 (2013), arXiv:1212.5241 [hep-ph]

# Impact of Scheme variation

Study effect of taking  $m_t^{\overline{\text{DR}}}$  instead of  $m_t^{\text{OS}}$



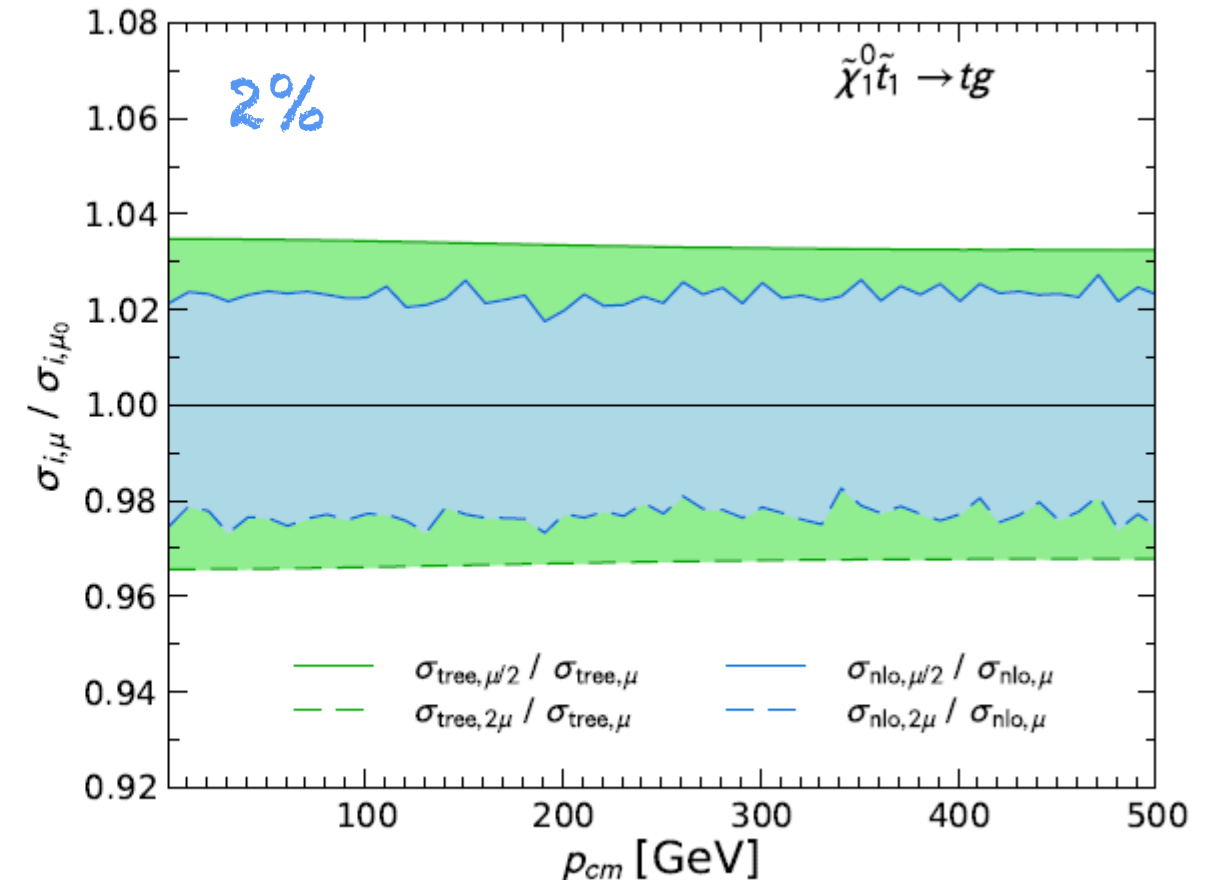
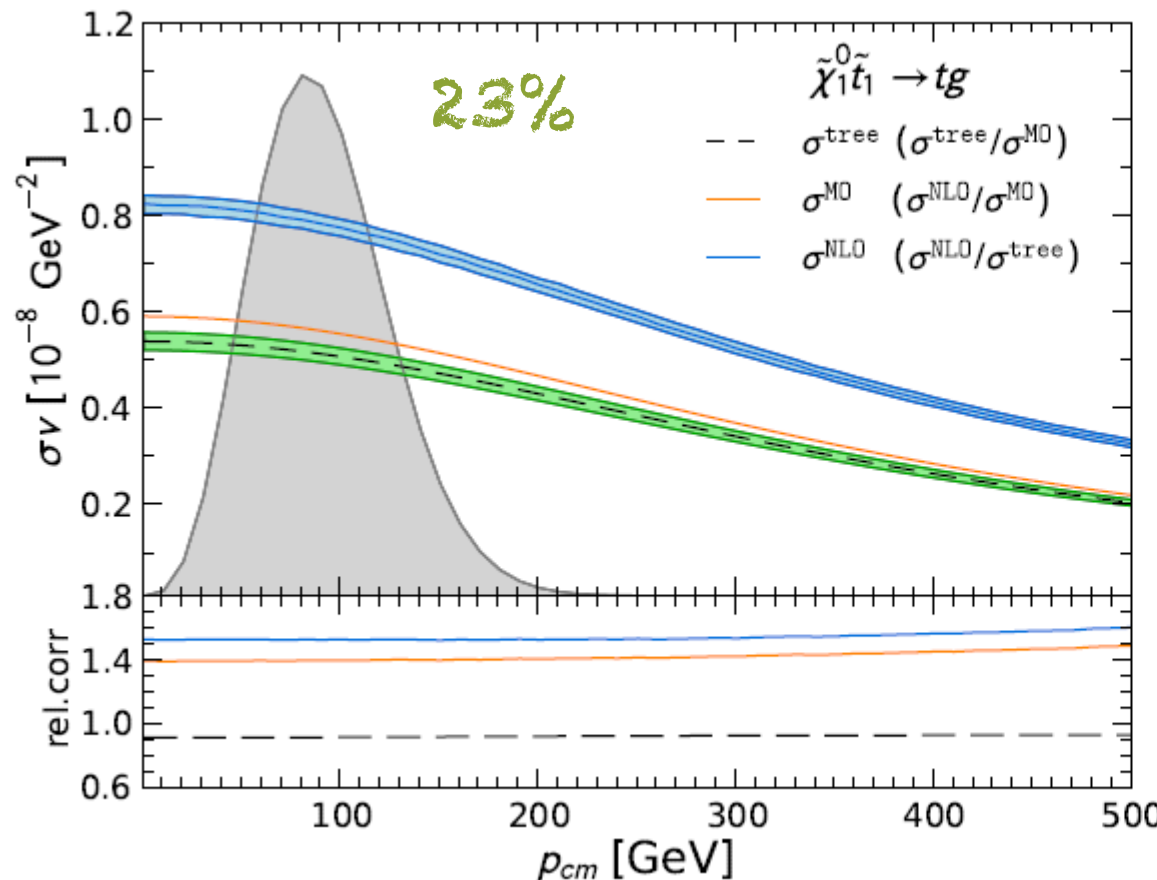
- MO larger than LO cross section as MO uses effective top mass
- Larger K-factor of 1.4 in contrast to our scheme with 1.05

→ confirms our choice of renormalisation scheme

J. Harz, B. Herrmann, M. Klasen, K. Kovařík, and P. Steppeler, Phys. Rev. D 93 114023 (2016), arXiv:1602.08103 [hep-ph]  
 J. Harz, B. Herrmann, M. Klasen, and K. Kovařík, Phys. Rev. D 91, 034028 (2015), arXiv:1409.2898 [hep-ph]  
 J. Harz, B. Herrmann, M. Klasen, K. Kovařík and Q. Le Bouc'h, Phys. Rev. D 87, 054031 (2013), arXiv:1212.5241 [hep-ph]

# Stop Coannihilation

Top gluon final state only process with QCD coupling at tree-level

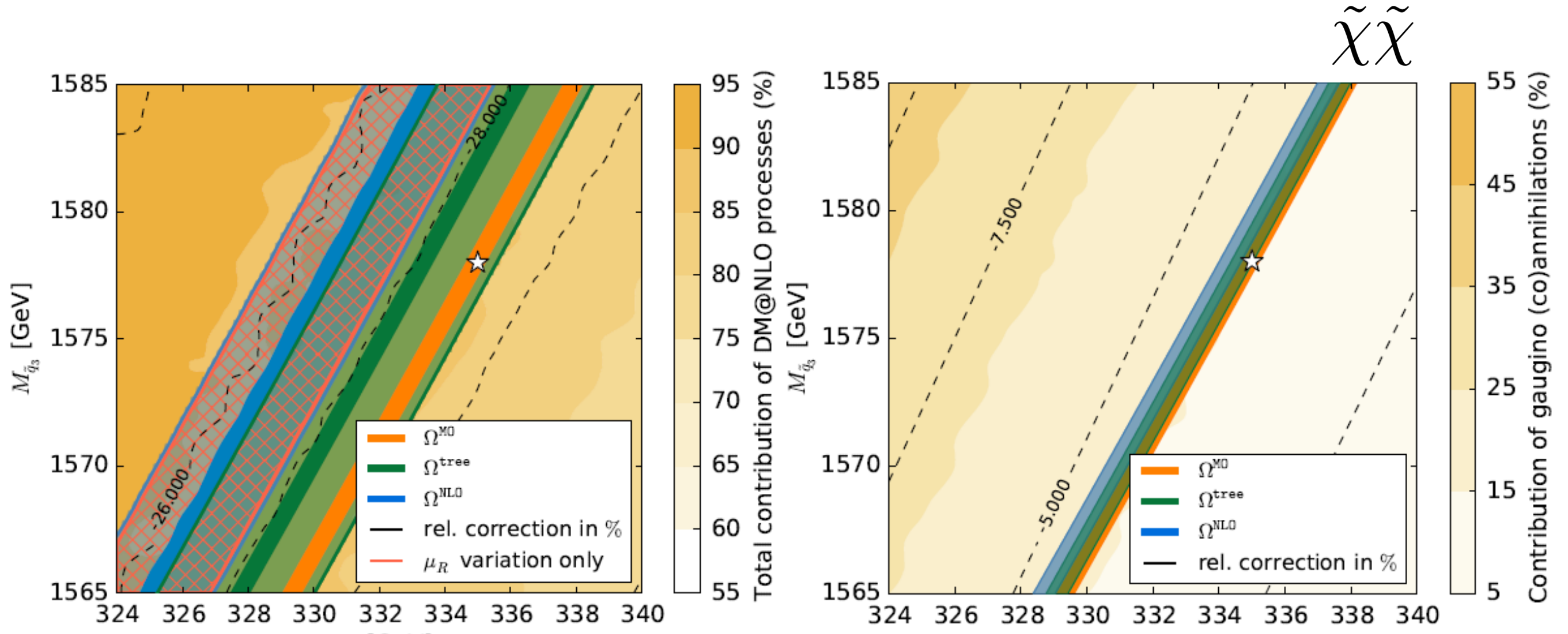


- Scale dependence on LO triggered already by  $\alpha_s$
- Scale dependence at NLO reduced to 2 %

→ K-factor of 1.5, correction of 40% w.r.t. MicrOmegas, 2 % theoretical uncertainty

J. Harz, B. Herrmann, M. Klasen, K. Kovařík, and P. Steppeler, Phys. Rev. D 93 114023 (2016), arXiv:1602.08103 [hep-ph]  
 J. Harz, B. Herrmann, M. Klasen, and K. Kovařík, Phys. Rev. D 91, 034028 (2015), arXiv:1409.2898 [hep-ph]  
 J. Harz, B. Herrmann, M. Klasen, K. Kovařík and Q. Le Bouc'h, Phys. Rev. D 87, 054031 (2013), arXiv:1212.5241 [hep-ph]

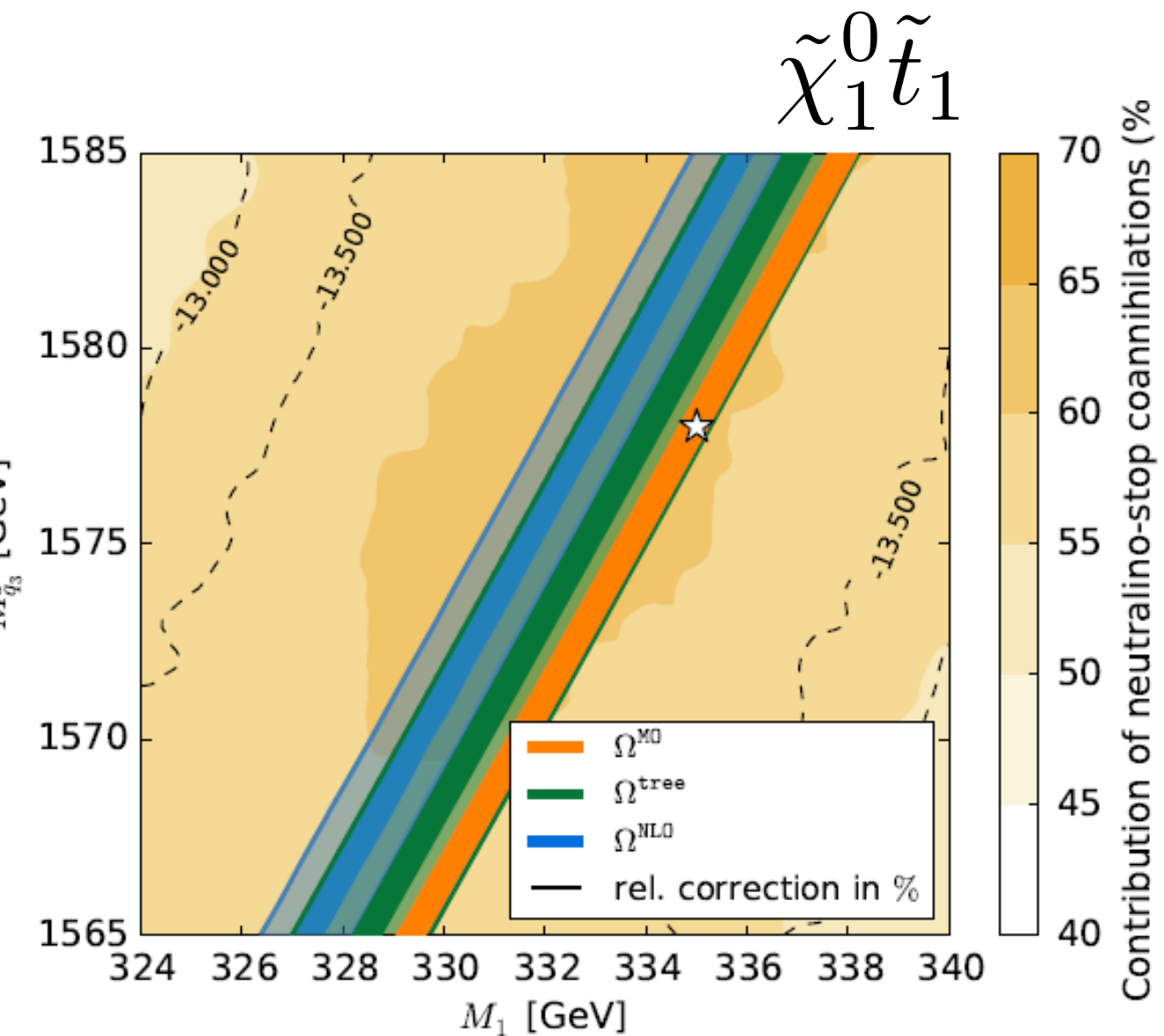
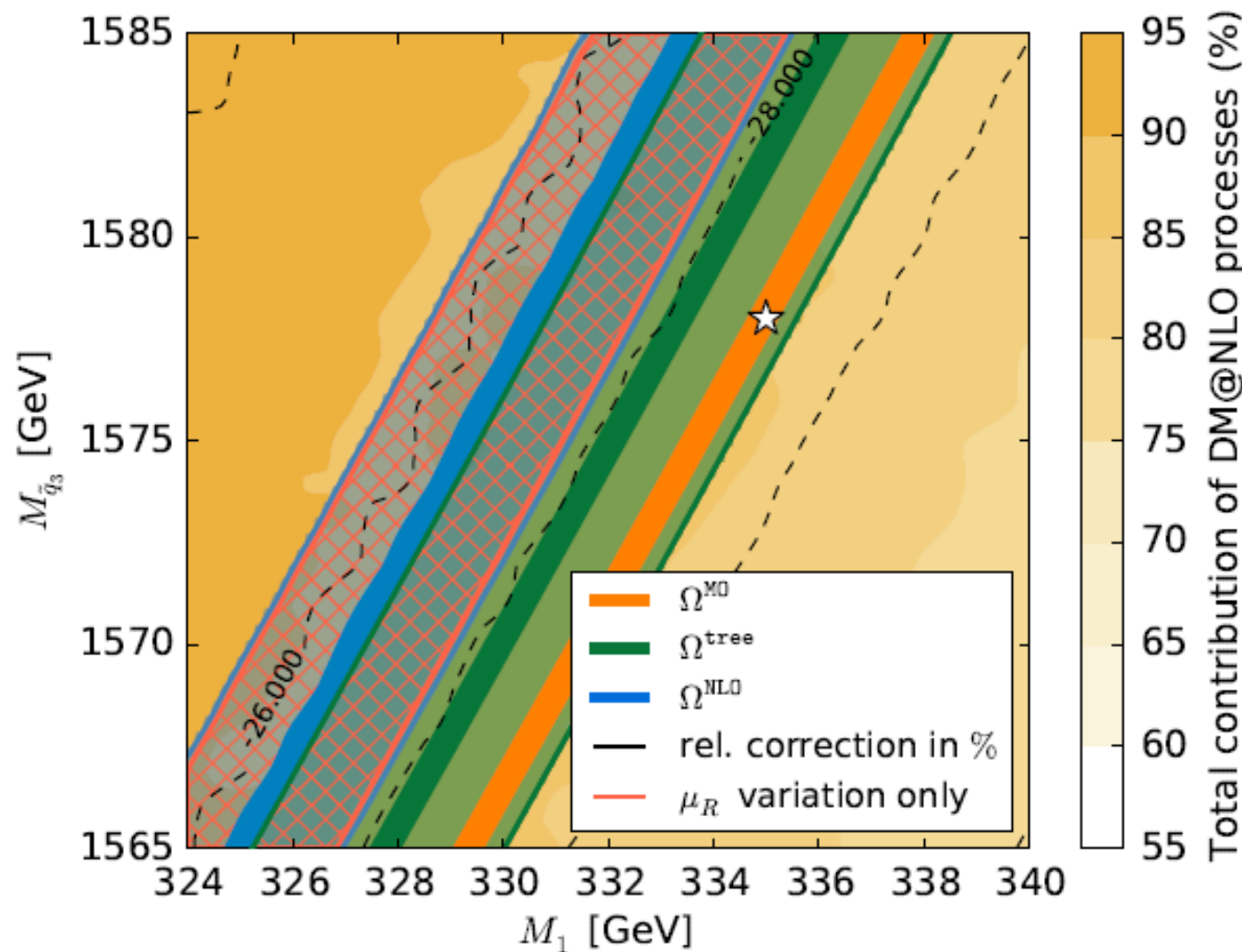
# Combined Scenario



- $\tilde{\chi}\tilde{\chi}$  • K-factor of 1.15, 5-10% correction w.r.t. MO, 5% scale uncertainty

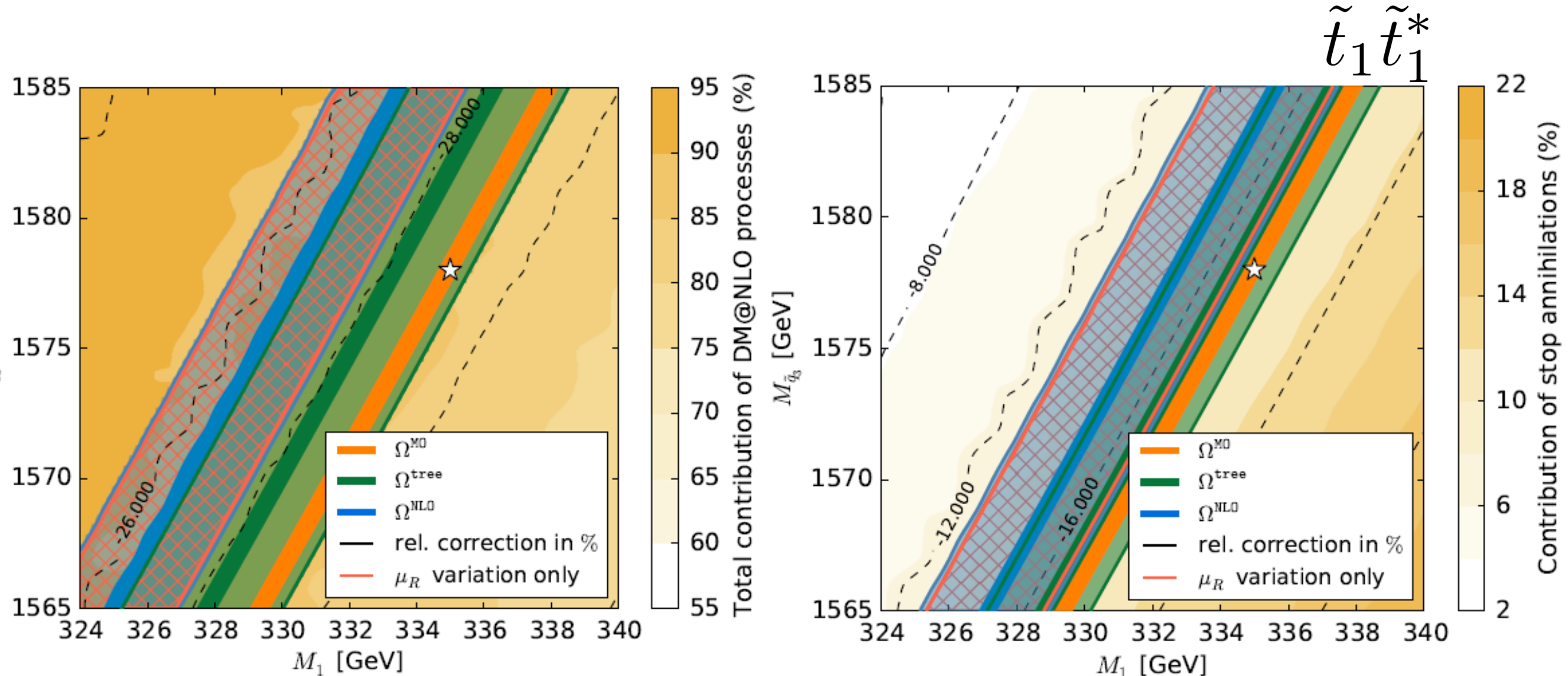
# Combined Scenario

$\tilde{\chi}_1^0 \tilde{t}_1$



- $\tilde{\chi}\tilde{\chi}$  K-factor of 1.15, 5-10% correction w.r.t. MO, 5% scale uncertainty
- $\tilde{\chi}_1^0 \tilde{t}_1$  K-factors of 1.05-1.5, 15% correction w.r.t. MO, 20% scale uncertainty

# Combined Scenario



- $\tilde{\chi}\tilde{\chi}$  K-factor of 1.15, 5-10% correction w.r.t. MO, 5% scale uncertainty
- $\tilde{\chi}_1^0 \tilde{t}_1$  K-factors of 1.05-1.5, 15% correction w.r.t. MO, 20% scale uncertainty
- $\tilde{t}_1 \tilde{t}_1^*$  K-factors of 1-9, up to 16% correction w.r.t. MO, 20% scale uncertainty

→ Correction of almost 30 % w.r.t. MO relic density calculation

# Conclusions

- current tools calculate relic density just at an (effective) tree level
- increased precision of theoretical relic density prediction by including SUSY-QCD corrections & Coulomb enhancement effects
- corrections can have significant impact of 10% - 60% depending on scenario
- first estimation of theoretical uncertainty coming from scheme and scale variations (scenario dependent!)
- we provide a library, linkable to MicrOMEGAs, for precise parameter studies and global fits



# Thank you!

